Pathways for Nitrogen Cycling in Earth's Crust and Upper Mantle: A Review and New Results for Microporous Beryl and Cordierite

Gray E. Bebout[1], Kris E. Lazzeri[2], and Charles A. Geiger[3]

[1]Department of Earth and Environmental Sciences, Lehigh University, Bethlehem, Pennsylvania, 18015, USA
[2]EA Engineering, Science and Technology, Inc., Layton, Utah 84041, USA
[3]Department of Materials Science and Physics, Section Mineralogy, Salzburg University, Hellbrunnerstrasse 34, A-5020 Salzburg, Austria

revised for *American Mineralogist* as an Invited Centennial Article (6-07-15)

ABSTRACT

Earth's atmosphere contains 27-30% of the planet's nitrogen and recent estimates are that about one-half that amount (11-16%) is located in the continental and oceanic crust combined. The percentage of N in the mantle is more difficult to estimate but it is thought to be near 60%, at very low concentrations. Knowledge of the behavior of N in various fluid-melt-rock settings is key to understanding pathways for its transfer among the major solid Earth reservoirs.

Nitrogen initially bound into various organic materials is transferred into silicate minerals during burial and metamorphism, often as NH_4^+ substituting for K^+ in layer silicates (clays and micas) and feldspars. Low-grade metamorphic rocks appear to retain much of this initial organic N signature, in both concentrations and isotopic compositions, thus in some cases providing a relatively un- or little-modified record of ancient biogeochemical cycling. Devolatilization can release significant fractions of the N initially fixed in crustal rocks through organic diagenesis, during progressive metamorphism at temperatures of ~350-550˚C (depending on pressure). Loss of fractionated N during devolatilization can impart an appreciable isotopic signature on the residual rocks, producing shifts in $\delta^{15}N$ values mostly in the range of +2 to +5‰. These rocks then retain large fractions of the remaining N largely as NH_4^+, despite further heating and ultimately partial melting, with little additional change in $\delta^{15}N$. This retention leads to the storage of relatively large amounts of N, largely as NH_4^+, in the continental crust. Nitrogen can serve as a tracer of the mobility of organic-sedimentary components into and within the upper mantle.

This contribution focuses on our growing, but still fragmentary, knowledge of the N pathways into shallow to deep continental crustal settings and the upper mantle. We discuss the factors controlling the return of deeply subducted N to shallower reservoirs, including the atmosphere, via metamorphic devolatilization and arc magmatism. We discuss observations from natural rock suites providing tests of calculated mineral-fluid fractionation factors for N. Building on our discussion of N behavior in continental crust, we present new measurements on the N concentrations and isotopic compositions of microporous beryl and cordierite from medium- and high-grade metamorphic rocks and pegmatites, both phases containing molecular N_2, and NH_4^+-bearing micas coexisting with them. We suggest some avenues of investigation that could be particularly fruitful toward obtaining a better understanding of the key N reservoirs and the more important pathways for N cycling in the solid Earth.

Keywords: nitrogen cycling, nitrogen isotopes, ammonium, microporous silicate, isotope fractionation, layer silicates, cordierite

INTRODUCTION

It is often thought that Earth nitrogen (N) resides entirely in the atmosphere and the biosphere, which together account for 27-30% of the total N budget. Many are surprised to learn that ~60% of the N resides in the mantle and that another 11-16% is stored in the continental and oceanic crust combined (see **Table 1**). In fact, the surface reservoirs of N receiving the most attention (i.e., ocean, soils, biosphere) contain far less than 1% of Earth's N by mass (**Table 1**; also see Bebout et al., 2013b). Despite its relatively inert and volatile behavior, N can occur in certain minerals in the crust and mantle, particularly when structurally bound as NH_4^+ (Bebout et al., 2013a; Busigny and Bebout, 2013). Ammonium-bound N in micas and feldspars (Eugster and Munoz, 1966; Honma and Itihara, 1981; Bos et al., 1988; Hall et al., 1996; Hall, 1999) is an efficient carrier of initially-organic N from surface reservoirs into the deep Earth at subduction zones and during formation of the continental crust. In the upper mantle, small amounts of N could be stored as NH_4^+ in silicate phases such as amphibole, phlogopite, clinopyroxene, and olivine (Yokochi et al., 2009; Watenphul et al., 2010) or as other species in diamond and various nitrides (e.g., TiN; Cartigny, 2005; Dobrzhinetskaya et al., 2009; see the discussion by Busigny and Bebout, 2013). Johnson and Goldblatt (2015) discuss the possibility that, in the deeper mantle, N is soluble in (Fe, Ni) alloy (see Roskosz et al., 2013).

Figure 1 illustrates key geologic reservoirs and sedimentary-organic pathways for N. The cycle begins with the incorporation of initially organic N into clays, during diagenesis, and involves the evolution of this N during prograde metamorphism, melting, and ultimately, melt

degassing during crystallization. It ends with the release of N back into the atmosphere. Diagenesis and metamorphism can provide for the addition of N to the mantle at subduction zones, by its release into fluids (see Bebout and Fogel, 1992), and the balance of this addition with the output of N via magmatism is important for understanding the long-term evolution of the mantle N reservoir (see Sano et al., 2001; Hilton et al., 2002). Study of N behavior in the deep-Earth (crust and mantle) has lagged behind investigations using other stable isotope systems (e.g., O, H, C, S). This is partly due to the difficulty in analyzing the N concentrations and isotopic compositions of silicate minerals and partly due the association of N with life resulting in greater attention from the biological community. As a result of these factors, knowledge of not only the sizes (**Table 1**), but also the isotopic compositions, of the important crust and mantle reservoirs is based on a relatively small number of studies (see Cartigny and Marty, 2013; Johnson and Goldblatt, 2015). In comparison, analyses of N in biological and soil/sediment systems abound because they can be made using less sensitive analytical methods often using highly automated modes (see Bebout et al., 2013b).

In this review article, we synthesize the present knowledge concerning the sizes and isotopic compositions of major crust and upper-mantle N reservoirs in the Earth and the key pathways among them. We stress that, because N can be retained in certain silicate phases, particularly those containing appreciable K^+ (i.e., layer silicates and feldspars), N can be retained to great depths in the continental crust and carried to even greater depths at subduction zones. We consider briefly the avenues for the incorporation of initially organic N into silicate materials (minerals and glasses) during diagenesis and seafloor alteration, as this process, followed by burial and subduction, largely governs the nature of the crust and upper-mantle N reservoirs. In this context, we also present new N isotope data for the microporous silicates beryl and

cordierite, and coexisting micas, and we discuss the implications of these results for N behavior during fluid-rock interactions and for the storage of N in the continental crust.

TECHNIQUES FOR ANALYSIS OF THE ISOTOPIC COMPOSITIONS OF NITROGEN IN SILICATES

Research relating to the behavior of N isotopes in silicate systems has largely been conducted by a small number of laboratories, owing to the trace concentrations of N in most rocks and minerals and the need to quantitatively release N from them (see the review by Cartigny and Marty, 2013). There are a few natural NH_4^+-rich silicate minerals such as buddingtonite ($NH_4AlSi_3O_8$; Erd et al., 1964; Barker, 1964) and tobelite ($(NH_4K)Al_2(Si_3Al)O_{10}(OH)_2$; Higashi, 1982), but most N tends to occur in the major rock-forming silicates at concentrations of several ppm to several thousand ppm (e.g., Honma and Itihara, 1981). Extraction of structurally bound N from silicate minerals and whole-rock samples in general requires heating for sustained periods of time at temperatures greater than about 1050°C, normally with some means of controlling redox conditions so that the speciation of the released N is known (see Cartigny and Marty, 2013). Heating can be accomplished by use of online furnaces similar to those used for noble gas measurements that allow stepped-heating or combustion experimentation (see Boyd et al., 1993; Pinti et al., 2007), in quartz tubes that are sealed at high vacuum and then heated in offline furnaces (allowing longer heating periods; see Bebout and Fogel, 1992; Boyd, 1997; Bebout and Sadofsky, 2004; Busigny et al., 2005a; Bebout et al., 2007), or via flash combustion in element analyzers that allow more rapid throughput (see Bräuer and Hahne, 2005; cf. Jia et al., 2003). Each of these methods has its advantages and disadvantages, but it is clear that any quantitative study of N concentrations and isotopic compositions in silicate systems must demonstrate that complete yields are obtained. Whereas some minerals and rocks appear to release most or all of

143 their N upon heating to such temperatures of 910 to 1000°C, higher temperatures or even melting
144 could be necessary for release of N from some materials (e.g., data for biotite separates in
145 Sadofsky and Bebout, 2000; results for buddingtonite in Bebout and Sadofsky, 2004).
146 Older techniques for analyzing N in silicate rocks and minerals include the Kjeldahl method,
147 employed by Haendel et al. (1986) and in other studies from that laboratory (e.g., Junge et al.,
148 1989). Bräuer and Hahne (2005) compared results obtained using the Kjeldahl method, element
149 analyzer techniques, and sealed-tube combustions followed by dual-inlet mass spectrometry.
150 They found that the sealed-tube combustion technique (see Sadofsky and Bebout, 2000) yields
151 results indistinguishable from those obtained via the Kjeldahl method, whereas the element
152 analyzer technique appeared to produce minor N fractionation arising from incomplete yields
153 that were obtained. Ammonium concentrations in micas and feldspar have also been measured
154 using IR spectroscopy, as demonstrated by Boyd (1997) and Busigny et al. (2004). This method
155 appears to produce good results comparable with those obtained by mass spectrometry (also see
156 the results for phengite, biotite, and tourmaline in Wunder et al., 2015).
157 Mass spectrometry measurements of the isotopic compositions of N_2 liberated by the various
158 extractions have been undertaken using gas-source instruments operated in either static or
159 dynamic modes, with the latter employing either dual-inlet (viscous flow) or carrier gas methods
160 using He (see discussion of these methods in Hashizume and Marty, 2005; Bebout et al., 2007;
161 Cartigny and Marty, 2013). Nitrogen isotope compositions are expressed as $\delta^{15}N_{air}$, which is
162 defined as:

163
$$\delta^{15}N = \left[\frac{(^{15}N/^{14}N)_{sample} - (^{15}N/^{14}N)_{std}}{(^{15}N/^{14}N)_{std}} \right] x10^{3}$$

where the standard (std) is the Earth atmospheric N_2 with isotopic ratio $^{14}N/^{15}N = 272$ (Mariotti, 1984)

CURRENT UNDERSTANDING OF NITROGEN PARTITIONING BEHAVIOR, SPECIATION IN FLUIDS, AND ISOTOPE FRACTIONATION IN SILICATE SYSTEMS

Partitioning of Nitrogen Between Fluid and Silicate Mineral Phases

The partitioning of N and its isotopes among minerals, fluids, and melts exerts a primary control over the evolution of all deep-Earth N reservoirs, in addition to governing the flux of N among the biosphere, atmosphere, and surface hydrosphere (see for example, recent discussion by Cartigny and Marty, 2013; Johnson and Goldblatt, 2015). It is reflected in the distribution of N among solid phases, and its speciation in these phases, and the degree to which N is stabilized in various molecules in fluids and melts. Busigny and Bebout (2013) provided a brief survey of the most significant N-bearing minerals, with an emphasis on the distribution of N in major rock-forming silicates in the crust and mantle (also see the more thorough discussion of other N-bearing silicate and non-silicate phases by Holloway and Dahlgren, 2002).

Honma and Itihara (1981) measured the NH_4^+ concentrations in coexisting minerals from various igneous and high-grade metamorphic rocks and proposed a hierarchy of NH_4^+ concentration, from most to least enriched, as: biotite > muscovite > K-feldspar > plagioclase feldspar > quartz. Biotite generally contains ~2.5x more NH_4^+ than coexisting muscovite (cf. Sadofsky and Bebout, 2000; cf. Boyd, 1997), ~3.7x more NH_4^+ than coexisting K-feldspar, and ~20x more NH_4^+ than plagioclase. This indicates that partitioning behavior is largely a function of the size of the interlayer sites in dioctahedral and trioctahedral micas and that NH_4^+ partitioning behavior into micas is similar to that for Rb^+, where both ions are slightly larger than

188 K^+ (i.e., 1.38 Å for K^+, 1.48Å for NH_4^+, and 1.52 Å for Rb^+; see Honma and Itihara, 1981).
189 Wunder et al. (2015) analyzed the NH_4^+ concentrations in coexisting minerals from a
190 metasedimentary rock (a high-P/low-T mica schist from the Erzgebirge, Germany) and
191 demonstrated that NH_4^+ concentrations in tourmaline can be roughly similar to those of phengite
192 in the same rock (i.e., biotite NH_4^+ = 1400 pm; phengite NH_4^+ = 700 ppm; tourmaline NH_4^+ =
193 500 ppm).
194 The speciation of N in fluid-rock systems is thought to be dependent on pressure,
195 temperature, redox conditions, pH, and the N content of the fluids (see the calculations by
196 Bottrell et al., 1988; Bakker and Jansen, 1993; Moine et al., 1994; Li and Keppler, 2014; Mikhail
197 and Sverjensky, 2014; discussion by Johnson and Goldblatt, 2015). The calculations of
198 Sverjensky et al. (2014) utilize a revised Helgeson-Kirkham-Flowers equation of state for
199 describing aqueous speciation for use at up to upper mantle *P-T* conditions (also see Pan et al.,
200 2013; Facq et al., 2014; Mikhail and Sverjensky, 2014). In crustal and subduction zone settings,
201 where $P \leq 3.0$ GPa and on which this contribution mainly focuses, the dominant fluid N species
202 is generally regarded as being N_2, with NH_3 being stable at reduced conditions. In silicate melts,
203 speciation of N is both temperature- and redox-dependent, and variations in speciation could
204 significantly affect N isotope fractionation during partial melting and crystallization (Libourel et
205 al., 2003; Roskosz et al. 2006; Mysen and Fogel 2010). Pöter et al. (2004) determined
206 experimentally NH_4^+ partitioning among muscovite, K-feldspar, and aqueous chloride solutions
207 in which the N was contained in NH_4Cl. Although it is difficult to use these results to predict the
208 partitioning and isotope fractionation in low-Cl systems, these experimental results show
209 partitioning of NH_4 among the three mineral phases largely consistent with the observations from
210 the natural suites (for the latter, Honma and Itihara, 1981; Sadofsky and Bebout, 2000).

Calculated Fractionation Factors

Nitrogen isotope fractionations have been calculated using vibrational spectroscopic data for several molecular species that are important for crust-mantle cycling, namely NH_4^+, NH_3, and N_2. The results of these calculations are shown in **Fig. 2a** (compiled by Busigny and Bebout, 2013). Disagreement in the calculations among several studies (Scalan, 1958; Richet et al., 1977; Hanschmann, 1981), particularly for fractionations involving N_2, suggests that further theoretical consideration is warranted, perhaps with improved spectroscopic data. It is evident though, in both Scalan's (1958) and Hanschmann's (1981) calculations, that N isotopic fractionation between NH_3 and NH_4^+ is far larger, at a given temperature, than that between N_2 and NH_4^+. Thus, redox conditions can greatly influence the degree of isotopic fractionation in fluid-melt-mineral systems. There is no evidence that coexisting NH_4^+-bearing minerals partition N isotopes differentially; however, there has been little work done on this topic. The only studies addressing this question demonstrated that there is no statistical difference in $\delta^{15}N$ values for coexisting biotite and muscovite occurring in amphibolite-grade metapelitic rocks (Boyd, 1997; Sadofsky and Bebout, 2000).

Results Relating to the Direction and Magnitude of Nitrogen Isotope Fractionation in Fluid-Rock Systems

For metasedimentary rock suites, increases in $\delta^{15}N$ with increasing grade, correlated with N losses, are consistent in direction and magnitude with an exchange between NH_4^+ in the silicates and N_2 in fluids, perhaps by a process approximating Rayleigh distillation (Haendel et al., 1986; Bebout and Fogel, 1992; Bebout et al., 1999a; Mingram and Bräuer, 2001; Busigny et al., 2003;

Mingram et al., 2005; Pitcairn et al., 2005; Jia, 2006; Bebout et al., 2013a). Kerrich et al., 2006 (see their Table 4 and Fig. 5) provide a good summary of the shifts in $\delta^{15}N$ values in metasedimentary rocks resulting from N loss during devolatilization. **Figure 2b** demonstrates that significant shifts in the $\delta^{15}N$ value of a residual N reservoir can occur via either a batch (straight line) or a Rayleigh distillation process. These isotopic shifts are strongly dependent on the temperature of the release of the N and its speciation (i.e., as NH_3 or N_2)—speciation of the fluid N as NH_3 produces far greater shifts because of the larger $10^3 ln\alpha$ associated with this exchange (see **Fig. 2a**). Based on the calculations in **Fig. 2b**, if N_2 is the dominant N molecular species in the fluid produced during devolatilization of sandstones and pelitic rocks, fluid N_2 with a range in $\delta^{15}N$ values of -2 to +6‰ could be expected. Indeed, analyses of the $\delta^{15}N$ of N_2 in fluid inclusion in quartz veins from low-grade metasedimentary exposures show values of -3 to +5‰ (Kreulen et al., 1982), -6.9 to -1.5‰ (Bottrell et al., 1988), and +3.7 to +4.0‰ (Bebout and Sadofsky, 2004). The range of $\delta^{15}N$ of -2 to +6‰ also largely overlaps the range characteristic for N_2 in natural gases (Müller et al., 1976; Jenden et al., 1988; Mingram et al., 2005). Pitcairn et al. (2005) noted a larger degree of fractionation at the highest grades of a metasedimentary suite in New Zealand showing a range in grade from nearly unmetamorphosed to upper amphibolite conditions. They proposed that this reflects a change in the speciation of N in the fluid phase from dominantly N_2 at the lower grades to dominantly NH_3 at higher grades.

Bebout and Sadofsky (2004), in another investigation of fluid-mineral N isotope fractionation behavior, measured the $\delta^{15}N$ of N_2 in fluid inclusions and NH_4^+ in biotite in one low-grade metamorphic quartz vein from Bastogne, Belgium (see Darimont et al., 1988; sample provided by J. Touret). The fluid inclusions contain ≥ 93 mole % N_2 and small amounts of CO_2 and/or CH_4, and the coexisting biotite contains 2280 ppm NH_4^+. Isotopic analyses of three samples of

the quartz in this vein yielded $\delta^{15}N$ values of +3.7, +3.9, and +4.0‰ for the N_2 in the fluid inclusions, and a single analysis of the NH_4^+ in the vein biotite yielded a $\delta^{15}N$ value of +6.8‰. The difference in $\delta^{15}N$ between the N_2 and the NH_4^+ (the mean $\delta^{15}N$ value for the fluid inclusions is +3.9‰, thus making the biotite-inclusion difference ~ +2.9‰) is similar to the $\Delta^{15}N_{NH_4^+-N_2}$ value calculated by Hanschmann (1981) for the petrologically inferred temperatures of formation of ~ 400°C (~ +2.8‰; see **Fig. 2a**). Analyses of N_2 and NH_4^+ in coexisting microporous silicates (i.e., beryl and cordierite) and micas, respectively, could provide another measure of the magnitudes and directions of isotopic exchange, as discussed later in this article.

PATHWAYS FOR NITROGEN CYCLING

Nitrogen in silicate-containing rocks largely derives from organic N, itself derived from atmospheric N via biologically mediated metabolic processes. The biological uptake of N, and its later transfer during diagenesis in near-surface or upper-crustal geologic environments into silicates such as clay minerals and their later metamorphic products, can ultimately give rise to a significant flux of surface N into deeper crustal and upper mantle reservoirs (see **Fig. 1**, modified after Boyd, 2001). In this section, we discuss the current understanding of the most important pathways for surface to deep-Earth N cycling.

Incorporation of Organic Nitrogen into Silicates During the Diagenesis of Sediments

Various low-temperature geologic processes at Earth's surface can lead to the incorporation of initially organic N into silicate phases. They, in turn, ultimately contribute to the entrainment of N to great depths, during burial and subduction. Low-temperature "mineralization" (i.e.,

devolatilization), the breakdown of organic material, releases N which is incorporated by authigenic clays such as illite, seemingly with little or no isotope fractionation (see Williams et al., 1989, 1995; Schroeder and McLain, 1998; Ader et al., 1998, 2006; Boudou et al., 2008; see the discussion in Thomazo et al., 2011). Although the bulk of the N in these diagenetically-altered sediments or metasedimentary rocks is held in clays or low-grade micas, and the organic matter is low-N kerogen, the whole-sediment/rock C/N and $\delta^{13}C$ and $\delta^{15}N$ values can resemble those of the sediment protoliths (see the example in Sadofsky and Bebout, 2003).

Nitrogen record of ancient biogeochemical processes: A number of recent studies have attempted to determine paleo-biogeochemical cycling behavior using the $\delta^{15}N$ of ancient sediments and low-grade metasedimentary rocks. Thomazo and Papineau (2013; also see Thomazo et al., 2011) provided a compilation of $\delta^{15}N$ values and other isotopic compositions, for a variety of Precambrian sedimentary materials of ages from 3.6 to 1.4 Ga. These authors discuss possible pitfalls in the interpretation of this record related to unknown effects of low-grade metamorphism on the N record, but suggest that any isotopic shifts due to metamorphism are likely to be small (i.e., <2.0‰). It appears that the greatest N loss and isotopic shifts in metamorphosed shales and sandstones occur during metamorphism over the temperature range of ~350-550˚C, depending on pressure (see Bebout and Fogel, 1992). In many cases N loss and isotopic shifts are related to the breakdown of chlorite and release of N from micas during the related dehydration of the rocks. Thus, low-grade metasedimentary rocks that experienced peak temperatures below ~350˚C likely preserve some information relating to paleo-biological processes.

Nitrogen Enrichment in Seafloor-Altered Basalts, Gabbros, and Ultramafic Rocks

Seafloor alteration of basaltic and gabbroic rocks can result in a significant enrichment of N, accompanied by isotopic shifts from "mantle-like" $\delta^{15}N$ values of -5 ± 2‰ to higher values approaching +10‰. The more elevated $\delta^{15}N$ values of these altered mafic rocks, in general, indicate the addition of a sedimentary-organic N component, presumably via pore fluids that previously exchanged with seawater and nearby sediment sections (see Busigny et al., 2005b; Li et al., 2007). Although a number of deep-sea basaltic sections sampled by drilling contain evidence for microbial activity in palagonitized glass (see Staudigel et al., 2008; Cockell et al., 2010), the effect of microbial processes on N enrichment is not understood (see Bebout et al., 2013b, manuscript in review).

The Metamorphic Devolatilization Pathway

Subduction-zone metamorphism: Retention of volatiles to great depths in subduction zones (for N, see **Fig. 3**) is known to be highly dependent on the thermal structure of the subduction margin. "Cool" margins allow volatile-rich rocks to transit through forearc regions with little or no devolatilization (see Bebout and Fogel, 1992; Busigny et al., 2003; Bebout et al., 2013a; Cook-Kollars et al., 2014; Collins et al., in press). A growing number of studies have investigated the deep subduction of N in the sediment, oceanic crust, and the hydrated upper mantle in down-going slabs.

Subducted sediments: Bebout and Fogel (1992) investigated N behavior during the well-characterized devolatilization history of the Catalina Schist, California, which was metamorphosed at 15-45 km depths in a paleoaccretionary complex (see **Figs. 4c, d**). It was shown that isotopically fractionated N was lost from units of the Catalina Schist that experienced relatively "warm" prograde *P-T* paths (i.e., epidote-amphibolite, EA, and amphibolite, AM; **Figs.**

4c,d). Based on the direction and magnitude of the isotope shifts, Bebout and Fogel (1992) proposed N_2-NH_4^+ exchange accompanying Rayleigh-like N losses during the metamorphism. In contrast, lower grade metamorphic units that experienced "cooler" prograde *P-T* paths (labeled LA, LBS, and EBS in **Figs. 4c,d**) apparently did not undergo significant devolatilization and related N loss (Bebout et al., 1999b). These latter units resemble their seafloor sediment protoliths in both whole-sediment $\delta^{15}N$ and the $\delta^{13}C$ values of reduced C (the latter representing metamorphosed organic matter). Sadofsky and Bebout (2003) documented similar preservation of protolithic C and N concentrations and isotopic compositions in low-grade metasedimentary rocks of the Franciscan Complex, California.

In two separate studies, Busigny et al. (2003) and Bebout et al. (2013a) investigated N behavior in the Schistes Lustres metasedimentary unit and associated UHP rocks at Lago di Cignana, NW Italy. The results indicate little or no loss of N during prograde metamorphism over a depth range of ~60 to 90 km (see **Figs. 4a, b**). The retention of N to ~90 km depth in subducted sedimentary rocks would imply the availability of this N for delivery to arc magma source regions or the deeper mantle. Bebout et al. (2013a) proposed some N loss, associated with a modest isotopic shift of perhaps 1-2‰ (see **Fig. 4a**), resulting from ~20% dehydration of the highest-grade metasedimentary rocks in this suite. Cartigny et al. (2001) analyzed N concentrations and $\delta^{15}N$ of microdiamonds from the Kokchetav (Kazakhstan) ultra-high pressure (UHP) marbles and "garnet-clinopyroxene rock," the latter presumably metabasaltic in composiiton, in a continental subduction setting. They proposed a metasedimentary source for the N in the diamond, based on the $\delta^{15}N$ values, implying retention of metasedimentary N to depths greater than 100 km. Here, the N was released into fluids during devolatilization reactions.

In the Catalina Schist amphibolite-facies unit, muscovite in metasedimentary leucosomes and sediment-sourced pegmatites has $\delta^{15}N$ values indistinguishable from those of muscovite in the migmatized metasedimentary rocks. This led Bebout (1997) to suggest that partial melting can occur without appreciable N isotope fractionation; however, further detailed work is required to test this hypothesis. The only other study of the behavior of N and its isotopes during migmatization is that of Palya et al. (2011), with Hall et al. (1996) presenting NH_4^+ concentration data only for a migmatite complex in Spain. The work by Palya et al. (2011), on the low-pressure migmatites at Mt. Stafford, Australia, is described in a later section.

Subducted metabasalts and metagabbros: Halama et al. (2010) and Busigny et al. (2011) considered the record of deep N subduction in basaltic and gabbroic rocks, focusing on the N concentrations and isotopic compositions in HP and UHP metamorphic suites. In the rocks investigated by Halama et al. (2010), N concentrations correlate positively with concentrations of K_2O, consistent with the proposal that N resides as NH_4^+ in phengite (no feldspar is present in these rocks). These authors subdivided these rocks into two groups, namely (1) those that retained significant amounts of N, with N concentrations overlapping those of seafloor basalts, and showing no evidence for metasomatic additions during subduction zone metamorphism, and (2) those that were enriched in N, and in many cases also the LILE and Pb (Bebout, 2007), from fluid-rock interactions during subduction. For the Mariana subduction margin, Li et al. (2007) estimated a N input flux of 5.1×10^6 g/km/yr N in oceanic crust, twice as large as the annual N input of 2.5×10^6 g/km in seafloor sediments subducting at the same margin.

Subducted ultramafic rocks: Philippot et al. (2007) and Halama et al. (2012) published N isotope analyses of subducted ultramafic rocks (from the Italian Alps and Spain) and, in general, were able to demonstrate that N in such rocks is carried to and retained at great depths, but at low

372 concentrations (mostly in the range of 1 to 8 ppm). The latter authors considered the significance
373 of this flux for the overall subduction input of N_2, and concluded that it is minor (see the range of
374 estimated input flux for this rock type in **Fig. 3**). However, at this point, it is difficult to estimate
375 the volume and N concentration of hydrated-slab ultramafic sections entering trenches and the N
376 budget in hanging-wall ultramafic rocks is also poorly constrained.

377 ***Efficiency of the arc volcanic return of subducted nitrogen:*** Subduction-zone cycling of N
378 encompasses many of the processes and pathways discussed in this paper, that is, low-
379 temperature surface incorporation of N into organic matter and volcanic glass, diagenetic
380 alteration, low- to high-grade metamorphism and devolatilization, and partial melting. The
381 subduction input flux of N, mostly as NH_4^+, can be compared with the output flux as molecular
382 N_2 in arc volcanic gases (see the discussion by Hilton et al., 2002). Several studies have
383 calculated the amount of N that is returned to Earth's surface via arc volcanism (**Fig. 3**; see
384 Hilton et al., 2002; Elkins et al., 2006; Fischer, 2008; Mitchell et al., 2010). In general, the
385 estimated "return efficiency" of N, that is, the arc volcanic N outputs compared to the trench N
386 inputs, ranges from ~15 to ~40%, but with considerable uncertainty. Still uncertain are the exact
387 geochemical mechanism(s) by which this N is transferred from subducting slab sections to the
388 overlying mantle wedge. Presumably this transfer occurs via aqueous C-O-H-S-N fluid or N-
389 bearing silicate melt, or some combination of these two types of fluids. It is unknown whether
390 this subarc release of N from slabs is accompanied by isotopic fractionation and the published
391 mixing models used to calculate arc-volcanic gas compositions do not consider this effect. In
392 general, it appears that the upper mantle experiences net N addition, largely through the
393 incorporation of NH_4^+ in various K-bearing mineral phases such as the micas (see the discussions
394 by Halama et al., 2010; Busigny and Bebout, 2013; Cartigny and Marty, 2013). Some studies of

the compositions of arc volcanic gases consider the possibility of shifts in the $\delta^{15}N$ values of deeply subducted rocks through N loss during devolatilization in forearcs (see Elkins et al., 2006). More recent isotopic work on arc volcanic gases has focused on individual, well-studied subduction zone segments for which the overall geometry and dynamics of the margin are well characterized (i.e., by geophysical studies) and where the subduction inputs are better characterized. The subduction inputs can be constrained by analyzing the N in seafloor sediments that are obtained by drilling outboard of the trenches (see Elkins et al., 2006; Mitchell et al., 2010; discussions by Sadofsky and Bebout, 2004; Li et al., 2007).

Other "regional metamorphism": Research has been conducted on the N behavior in regionally metamorphosed rock suites that are not observably related to subduction, where a number of them are associated with continental collision. An early example is presented in a series of papers on N mobility in metamorphic rocks from the Dome de L'Agout, France, an extensional gneiss dome, in which the authors stressed the importance of NH_4^+ in micas (Kreulen and Schuiling, 1982; Duit et al., 1986). It was proposed that the release of N was related to the retrograde replacement of biotite by chlorite, where the latter layer silicate is unable to incorporate significant amounts of NH_4^+ (Duit et al., 1986; cf. Visser, 1992). Sadofsky and Bebout (2000) documented the retention of initially organic N in amphibolite-facies, medium-P/T facies series rocks at the Townshend Dam exposure in Vermont. The work focused mostly on analyses of mica separates (also see the study of very NH_4^+-rich white mica in schists from the Betic Cordillera by Ruiz Cruz and Sanz de Galdeano, 2008). Low-grade equivalents to the Townshend Dam rocks were not available for comparison study; however, these rocks could well have lost appreciable fractions of their initial N contents at grades lower than those now represented at this exposure. Jia (2006) studied the N behavior for greenschist- to amphibolite-

418 facies metamorphism in the Cooma metasedimentary suite, Australia. Here, N loss at
419 temperatures from 350 to 600˚C was accompanied by modest isotopic shifts that were consistent
420 with a Rayleigh or batch distillation process and speciation of N in the fluid as N_2 (see **Fig. 2b**).
421 In contrast, Jia invoked NH_3-NH_4^+ exchange at temperatures of 650 to 730˚C during the higher-
422 grade migmatization to account for far larger positive shifts in $\delta^{15}N$ in the high-grade rocks.
423 Plessen et al. (2010) examined N concentrations and N isotopic compositions for a suite of
424 greenschist- to amphibolite-grade metasedimentary rocks in western Maine, USA. They
425 documented moderate loss of N in the higher-grade rocks, accompanied by some shift in $\delta^{15}N$.
426 Plessen et al. analyzed both whole-rocks and biotite separates and discussed the effect of
427 changing redox conditions on N_2-NH_4^+ and NH_3-NH_4^+ exchange during the metamorphic
428 devolatilization. Mingram et al. (2005) investigated the N loss and associated isotopic shifts in a
429 Paleozoic sediment section presumed to be the source of natural gases in the North German
430 Basin containing up to ~90% N_2 (also see Krooss et al., 2005). The former authors suggested that
431 the bulk of the released N was dissolved as NH_3/NH_4^+, in saline pore fluids, which was then
432 oxidized to produce N_2 in the natural gases. As a final example of a study of regionally
433 metamorphosed rocks in a collisional subduction setting, Li et al. (2014) proposed that
434 anomalously low $\delta^{15}N$ values in micas from UHP metaigneous rocks of the Sulu orogenic belt,
435 China, indicate abiotic N reduction arising from near-surface fluid-rock interactions during the
436 Neoproterozoic Era.

437 **Contact metamorphism:** Contact metamorphic aureoles can provide clear records of
438 mineral reaction history, with well-defined heat sources. However, the transient nature of the
439 heating can lead to significant kinetic effects that hinder the attainment of mineral equilibration
440 and the growth of large crystals. Bebout et al. (1999a) investigated, as an example, the Skiddaw

Aureole (English Lake District), selected in part because of the very homogeneous whole-rock compositions of the metapelitic wall-rocks. This homogeneity simplified the determination of the fraction of N lost due to devolatilization that occurred during contact metamorphism. In the Skiddaw Slate wall rocks, the K_2O concentration is very uniform and the measured decrease in N concentration toward the igneous contact is associated with a loss of N from micas, which are the most important mineral hosts for the N (as NH_4^+). Although the rocks metamorphosed near the contact were variably overprinted by retrograde fluid-rock interactions, they show a clear shift to higher $\delta^{15}N$ values that was associated with N loss at the higher grades.

In the Karoo Basin, South Africa, heating by a series of basaltic sills at depth metamorphosed a sedimentary section, devolatilizing the sediments and producing explosive hydrothermal venting (see Svensen et al. 2008). Abundant buddingtonite was produced by this hydrothermal activity, where it acted as a cement. Study of metamorphosed rocks directly adjacent to one of these sills showed changes in N concentrations and $\delta^{15}N$ values similar to those observed for the Catalina Schist and Skiddaw Aureole. The $\delta^{15}N$ values of the N_2 which was produced by devolatilization of the Karoo Basin sediments (+1.75 to +6.0‰), are similar to those calculated for buddingtonite that crystallized during the hydrothermal fluid venting.

Nitrogen Metasomatism and the Formation of Ore Deposits

An investigation of the metasomatic rocks of the Catalina Schist (Bebout and Barton, 1993; Bebout, 1997) demonstrated the utility of N as a tracer of fluid-rock interactions and, in particular, the fluid-mediated transfer of initially organic N at depth. Here, N of metasedimentary origin is enriched in a variety of metasomatized rocks, for example, blueschist-facies-metamorphosed conglomerate cobbles, veins and their envelopes, and pegmatites. In all of these metasomatized rocks, N enrichments mirror those of K_2O, again demonstrating the ability of

NH_4^+ to substitute for K^+ in certain silicates. **Figure 5** shows this correlation for the blueschist-grade conglomerate cobbles (data from Bebout, 1997). Other LILE, specifically Cs, Rb, and Ba, show enrichments positively correlated with those of N and K_2O. The $\delta^{15}N$ values of these cobbles are very uniform and identical to those of other metasomatic rocks in this unit and the blueschist-facies metasedimentary rocks (Table 2 in Bebout, 1997), the latter presumed to be the source of the N.

Another example of the behavior of N and its isotopes during metasomatic processes is found at an exposure of subduction-related metabasaltic rocks in the Tianshan, China. **Figure 6** shows variations in the concentrations of N and several other trace elements across a vein envelope in which blueschist-grade metabasaltic rocks are transformed to eclogite toward the contact with the vein (from Halama et al., manuscript in preparation; see description in Beinlich et al., 2010; sketch from that paper in **Fig. 6d**). Samples collected along a traverse of this envelope show correlated losses in N and the LILE (K, Rb, and Ba; see **Figs. 6a-c**), reflecting the destabilization of phengite during eclogitization. The N loss during eclogitization occurred with little or no change in $\delta^{15}N$ except in the vein itself. For the same traverse, John et al. (2012) modeled the diffusion of Li and its isotopes and proposed a very short-duration fluid-rock event to produce the observations.

In veins from various settings, the presence of NH_4^+-bearing minerals (commonly micas) and N_2 in fluid inclusions (Duit et al., 1986; Darimont et al., 1988; Ortega et al., 1991; Visser, 1992; Andersen et al., 1993) indicate the mobility of N in fluids during metamorphism, in some cases with the fluid producing ore deposits. Kerrich et al. (2006) measured N concentrations and isotopic compositions of muscovite in hydrothermal veins containing appreciable Au. They argued that the fluid flow that produced the veins originated from a sedimentary source (also see

Jia et al., 2003). Pitcairn et al. (2005) also investigated the mobilization of metasedimentary N into ore-forming fluids, assessing fluid-rock fractionation behavior during devolatilization of the sources. Krohn et al. (1993) examined enrichments of NH_4^+ (some of it in buddingtonite) in shallow-crust hydrothermal systems utilizing near-infrared spectroscopy. Because of the high NH_4^+ content in these hydrothermal systems, their close association with Hg, and the small crystal size of the NH_4^+-bearing minerals, they proposed that NH_4^+ is transported by a late-stage vapor phase or as an organic volatile. As a further example of NH_4^+ enrichment occurring during magmatic hydrothermal processes, Bobos and Eberl (2013) described NH_4^+-illite-rich altered andesites associated with sub-volcanic diorite emplacement and crystallization.

As noted above, Bebout et al. (1999a) documented loss of N in the contact aureole developed at the margins of the Skiddaw Granite and the addition of this N to the cooling intrusive, where it was concentrated in a greisen (see another study of N in ore-deposit greisen by Junge et al., 1989). The $\delta^{15}N$ values of the Skiddaw greisen, which is associated with the tin-tungsten deposits at the Carrock Fell Mine, are consistent with an up-temperature flow of a N-bearing fluid from the wall rocks undergoing devolatilization into the granite.

Anatexis in the Continental Crust

Little work has been conducted on migmatites, leucosomes, and pegmatites aimed at understanding the nature of mineral-melt partitioning and possible melting-related isotopic fractionation of N. Palya et al. (2011) investigated the behavior of N for a series of partial melting reactions in the Mt. Stafford migmatite suite and demonstrated strong retention of N in these rocks despite extensive melting at ~2.0-4.0 GPa (**Fig. 7**). At lower metamorphic grades, muscovite and biotite were presumed to be the dominant N reservoir. However, as the two micas

were destabilized during dehydration melting reactions, N was partitioned into K-feldspar and significant amounts of N were retained in cordierite presumably as molecular N_2 (see the discussion below). Cordierites in the higher-grade rocks at this locality (Zone 4) contain 118-351 ppm N (see **Fig. 8** and Table 4 in Palya et al., 2011). The following outlines a series of reactions experienced by these rocks (from Vernon et al., 1990, and White et al., 2003; *with the likely N-bearing minerals in italics*):

Zone 1:

Ms + *Bt* (unmelted protolith/equivalent)

Zone 2:

Ms + Qtz → And + *Kfs* + H_2O

Kfs + *Bt* + *Crd* + Qtz + H_2O → leucosome ± (Qtz – *Kfs* – *Bt*)

Kfs + Qtz + *Bt* + H_2O → And + leucosome ± (Qtz – *Bt* – *Kfs*)

Zone 3:

Bt + Sil + Qtz → Spl + *Crd* + leucosome ± (*Kfs* – Qtz – H_2O)

Bt + Spl + Qtz → Grt + *Crd* + *Kfs* + melt

Zone 4:

Grt + *Bt* + Qtz → Opx + *Crd* + *Kfs* + melt

Although some N loss from these rocks with increasing grade is evident (see **Figs. 7a, b**), isotopic shifts associated with this loss appear modest (with a subset of the Zone 4 samples having $\delta^{15}N$ values greater than +7‰), indicating only minor isotopic fractionation during the partial melting.

Buildup of the Nitrogen Reservoir in the Continental Crust during the Precambrian (and its Present State)

Uptake of N via biological processes, and the gradual transfer of this N to the crust and mantle, are thought to be important in the evolution of the early-Earth atmosphere (Boyd, 2001; Goldblatt et al., 2009). Like the subduction pathway (**Fig. 3**), this avenue for incorporation into and storage in the continental crust involves much of the process laid out in **Fig. 1**. This begins with the biological uptake of N from the atmosphere/hydrosphere, proceeding through diagenesis and then low- to high-grade metamorphism and ultimately deep-crustal partial melting. Goldblatt et al. (2009) proposed that halving the amount of atmospheric N_2 reservoir by biological fixation, through a net reaction of the type $N_2 + 3H_2O \rightarrow 2NH_3 + 1.5O_2$, would have resulted in the production of large amounts of O_2 for addition to the atmosphere. The sequestering of biological N into clays at or near Earth's surface, and with time further into deeper crustal rocks (where it could be stored), would have prevented N return to the atmosphere.

A better understanding of the concentrations and $\delta^{15}N$ values of the continental crust will require further investigation of the various volumetrically important crustal rocks (see the discussion by Johnson and Goldblatt, 2015). Several observations can be made. The N concentrations for crustal rocks at Mt. Stafford (Palya et al., 2011; see **Figs. 7a, b**), for example, are generally considerably higher than the estimated average continental crust concentration of 56 ppm (see Rudnick and Gao, 2014). Bach et al. (1999) determined N concentrations, but no isotopic compositions, for rocks from the KTB drill hole, in Oberpfalz, southern Germany, which sampled a 7 km section of crystalline basement metamorphosed during the Variscan orogeny. They noted a general positive correlation between whole-rock N concentration and biotite modal abundance and, thus, higher concentrations of N in paragneisses compared to

556 metabasites. Nitrogen concentrations measured along the drilled section ranged from ~5 to 50
557 ppm, lower than the 56 ppm average for the bulk-continental crust (see Rudnick and Gao, 2014).
558 Based in part on a consideration of K/U ratios, Cartigny et al. (2013) suggested 2.5 to 5 times the
559 amount of N in upper continental crust estimated by Rudnick and Gao (2014) using the data
560 compilation by Wlotzka (1972; also see the larger estimate by Johnson and Goldblatt, 2015).
561

562 **THE MICROPOROUS SILICATES BERYL AND CORDIERITE: NEW RESULTS ON THEIR NITROGEN**
563 **CONCENTRATIONS AND ISOTOPIC BEHAVIOR**
564

565 Up to now, most study of rock-forming minerals that can contain N has focused on layer
566 silicates and feldspar, where N occurs in the NH_4^+ ion. There is, however, another class of
567 minerals, namely microporous silicates that can contain charge-neutral molecules or gases, and
568 here specifically N_2, in their structures (Armbruster, 1985). They may serve as another crustal
569 sink for N. In this section, we present new mass spectrometry results on the N concentrations and
570 isotopic compositions in microporous beryl and cordierite. In addition, in several cases, we
571 measured the N concentrations and isotopic compositions for coexisting muscovite and biotite in
572 order to better understand the fractionation behavior of N between microporous and layer
573 silicates (data are from Lazzeri, 2012).

574 Cordierite with the idealized composition $(Mg,Fe)_2Al_4Si_5O_{18}\cdot[H_2O, CO_2, N_2\ldots]$ is
575 commonly found in Al-rich metamorphic rocks such as metapelites (Schreyer, 1965; also see
576 Kalt et al., 1998) and also certain igneous rocks (Clarke, 1995), including pegmatites (Heinrich,
577 1950). Beryl with the ideal composition $(Al_2Be_3Si_6O_{18})\cdot[H_2O, CO_2, N_2\ldots]$ is typically found in
578 granites or granite pegmatites (London and Evensen, 2002), but it can also occur in certain mafic
579 metamorphic rocks and low- to high-temperature hydrothermal veins. A few studies have

580 investigated the presence of N_2 in cordierite and its concentration (e.g., Lepezin et al., 1999;
581 Geiger et al., in preparation), but very few data exist on its molecular isotopic compositions (see
582 the small dataset for beryl presented in Scalan, 1958). The results for cordierite, a rock-forming
583 mineral, have implications for the storage of N at shallow to mid-levels of the continental crust,
584 because metamorphosed pelites can occur in geologically large amounts.

585 Nearly all naturally occurring cordierites occur as the lower-temperature ordered
586 orthorhombic modification and not the hexagonal "high" form with its disordered Al-Si
587 distribution. Beryl is isostructural with "high" cordierite. The crystal structures of cordierite and
588 beryl are similar because both contain structural rings consisting of six corner-sharing $(Si/Al)O_4$
589 tetrahedra that are cross-linked by octahedra and Al/BeO_4 tetrahedra, thereby forming a three-
590 dimensional framework. These rings of corner-shared tetrahedra are stacked one over another
591 producing infinite one-dimensional channelways running parallel to the *c*-axis (**Fig. 9**). The rings
592 form 'bottlenecks' with a diameter of about 2.8 Å and, in their middle, alkali cations (Na and K
593 for cordierite and these elements as well as Cs for beryl) can be found at relatively low
594 concentrations (e.g., Armbruster, 1986). Single, free molecules such as H_2O, CO_2, N_2, CO, O_2,
595 and H_2S and neutral atoms like Ar and He can be located in structural cavities or pores located
596 between the bottlenecks (Damon and Kulp, 1958; Armbruster, 1985; Kolesov and Geiger, 2000).
597 The molecules can be incorporated during crystallization, but they can, to unknown extents,
598 move in or out with changing *P-T-X* conditions. The presence of alkali cations within the rings
599 can act to slow or block diffusion of the molecules in or out of the channels. The dominant
600 molecular channel constituents in cordierite are H_2O (up to 3.8 wt %) and CO_2 (up to 2.2 wt %)
601 and the former for beryl. Both molecules have received considerable attention and different types
602 of crystallographic, mineralogical, and geochemical study and, thus, their behavior is fairly well

603 understood. The concentrations and isotopic behavior (i.e., geochemical) of the less abundant
604 molecular species N_2, CO, O_2, H_2S, Ar and He are not well documented.
605 In the case of cordierite, degassing experiments reveal that N_2 is probably the third-most
606 abundant species in many crystals, suggesting that N_2 may play an important role in the fluids
607 from which they crystallized (Geiger et al., in preparation). Indeed, fluid inclusion studies of
608 granulites and eclogites confirm the presence of N_2-bearing metamorphic fluids at elevated
609 temperatures and pressures (Andersen et al., 1990, 1993; Kreulen and Schuiling, 1982; Touret,
610 2001). In addition to N_2, a couple of studies have proposed the presence of minor amounts of
611 NH_4^+ and NH_3 within the channels of both cordierite and beryl (Mashkovtsev and Solntsev,
612 2002; Bul'bak and Shvedenkov, 2005), but more work is needed in this direction.
613 The concentrations and isotopic compositions of N occluded in cordierite and beryl are
614 believed to depend on several factors (see Geiger et al., in preparation): (1) the temperature and
615 pressure during crystal growth, (2) crystal-chemical and molecular properties, (3) the
616 composition of the coexisting fluid present, and (4) fractionation effects of N within the fluid.
617

618 **Continuous Heating and Mass Spectrometry on Cordierites to Determine their Occluded**
619 **Molecular Species**

620 Geiger et al. (in preparation) studied a number of cordierites from a wide range of petrologic
621 environments using continuous heating experiments from 25 to 1400 °C with a coupled
622 quadrupole mass spectrometer (see **Supplementary Fig. 1**). The aim of the study was to
623 determine *all* types of molecular species, both major and minor, that can be occluded in
624 cordierite, their temperature release behavior and, in some cases, their concentrations. The
625 experimental method discriminates between molecular species by their mass-to-charge ratios

(*m/z*). Both N_2 and CO are characterized by *m/z* = 28 and thus their peaks overlap in the mass spectrometry profiles. N_2 can be discriminated from CO by elevated *m/z* 28:44 ratios, indicating that a peak at *m/z* 28 cannot be solely explained by secondary CO^+ fragments produced from occluded CO_2 molecules. In order to test for the presence of a N_2 molecule, one can also use the species *m/z* 14, which can be assigned to the fragment N^+.

Based on a large number of degassing experiments of different cordierites, it was shown that the most N_2-rich cordierites are those from the granulite facies. Cordierites from medium-grade amphibolite-facies rocks contain less N_2, and pegmatite samples show the least amounts of N_2 of all the samples studied. These observations are confirmed by the stable isotope extraction measurements made on some of the samples, described below. The results also confirm the work of Lepezin et al. (1999) and their conclusions, showing that the concentration of N_2 in cordierite generally increases with increasing metamorphic grade (these authors did not measure N in cordierite from pegmatites). Finally, these degassing experiments demonstrate that the heating of cordierite (and beryl) to temperatures of 1100 ˚C, for three hours, should be sufficient to expel all molecules from their structural channels (see the examples of the release spectra in **Supplementary Fig. 1**).

Methods for Isotope Ratio Mass Spectrometry on Nitrogen in Cordierite and Beryl

Following upon the continuous heating measurements discussed above, heating experiments using the sealed-tube and mass spectrometry methods of Bebout et al. (2007) were undertaken to determine the N release characteristics for cordierite and beryl and the optimal heating regimen to obtain complete extraction of N for isotopic measurements. As a test, an inclusion-free beryl crystal, as examined by petrographic examination, was crushed and sieved to produce three

649 grain-size fractions: 0.125-0.25 mm, 0.25-0.50 mm, and 0.50-1.0 mm. Approximately 60 mg of
650 each size fraction were loaded into 6 mm o.d. quartz tubes together with 1 g of CuO_x reagent and
651 evacuated for 24 hours, with intermittent heating to ~100°C with a heat gun before sealing. The
652 sealed tubes were heated in a furnace at a controlled rate to either 1050 or 1100°C and for
653 varying periods of time between 180 to 300 minutes. An analysis of the results for these
654 differently-sized separates showed no difference outside analytical uncertainties in their
655 N concentrations or $\delta^{15}N$ values of ~36 ppm and +5.3‰. A number of recent studies have
656 concluded that quantitative extraction of N is accomplished for a wide range of metasedimentary,
657 basaltic, and ultramafic rocks at temperatures of 1000˚C (Bebout et al., 2007; Busigny et al.,
658 2005b; Halama et al., 2010; Li et al., 2007). However, N extraction from some mineral separates
659 can require higher temperatures (e.g., biotite; see Sadofsky and Bebout, 2000). Following this
660 test experiment on beryl, all further extractions were undertaken by heating to 1100˚C for 180
661 minutes, using the heating and cooling regimen of Bebout and Sadofsky (2004) and Bebout et al.
662 (2007). The extracted N_2 was purified in an all-metal extraction line. It was then transferred into
663 a Finnigan MAT 252 mass spectrometer via a Finnigan Gas Bench II and a U-trap interface
664 where small samples of N_2 (~50-200 nmoles) were entrained into a He stream.
665 Clear, gem-like beryl and cordierite crystals (**Appendices A and B**) were used in all
666 experiments in order to minimize the possibility of contamination from tiny mica inclusions
667 potentially containing NH_4^+. The lack of mica inclusions was also confirmed using petrographic
668 methods. A number of the cordierites were also characterized for their channel contents in the
669 degassing experiments of Geiger et al. (in preparation; see **Supplementary Fig. 1**). Samples
670 were crushed and sieved to reach a grain size of 0.25-1.0 mm and cleaned with purified water

and an acetone solution. For these extractions, aliquots of cordierite and beryl (17-116 mg) or mica (10-40 mg) were loaded into the quartz tubes with 1 g of CuO_x reagent.

Nitrogen Concentrations and $\delta^{15}N$ Values of Cordierite from Various Geological Settings

The N concentrations and $\delta^{15}N$ values for thirty cordierite samples, eight of these with coexisting biotite, are listed in **Table 2**. The results are shown in **Figs. 8 and 9**. The cordierites show a large range of N concentrations, from 5 to 4525 ppm, with most containing less than 1500 ppm N. $\delta^{15}N$ values range from +1 to +17‰. **Figure 8a** shows that the N concentration generally increases with increasing metamorphic grade. Cordierites from granulites, including Mt. Stafford, tend to contain more N, and have lower $\delta^{15}N$, than cordierites from medium-grade metamorphic rocks. The simplest interpretation for this observation is that NH_4^+ held mostly in mica (muscovite and biotite) at lower grades is liberated at higher metamorphic temperatures through various dehydration reactions. Nitrogen is released into the fluid phase, speciated as N_2, then incorporated into cordierite. The N released from the micas is expected to have $\delta^{15}N$ lower than that of the NH_4^+ in the micas (see **Fig. 2b**), thus explaining the lower $\delta^{15}N$ for N_2 in the cordierite channels.

It should be noted that pegmatitic cordierites have N concentrations of less than 70 ppm, which fall toward the lower end of the observed concentration range for all cordierites. Their $\delta^{15}N$ values are similar to those for cordierite in medium-grade metapelites. $\delta^{15}N$ values for the various cordierite samples range from +1 to +12‰, overlapping the $\delta^{15}N$ range characteristic for organic N, with the exception of sample CL-177-1 (+30‰) and Wards (+16‰; see **Table 2**).

Nitrogen Partitioning Behavior Between Coexisting Cordierite and Biotite

Biotite in pegmatites has N concentrations of 70 to 134 ppm higher than those of the coexisting cordierites, but to varying degrees (see **Fig. 9**). In two of the three experiments, the $\delta^{15}N$ values (+1.8 to +11‰) of the biotites are lower than the values for cordierite from the same rock sample (**Fig. 9**). In the third case, the $\delta^{15}N$ values for the coexisting minerals are similar. For two granulite facies rocks, biotite has N concentrations of 65 and 116 ppm and they are lower than those of the coexisting cordierites with concentrations of 162 and 232 ppm N, respectively. For three rock samples whose origins are uncertain ("uncategorized"), cordierites have N concentrations and $\delta^{15}N$ values higher than those of coexisting biotite. Thus, the partitioning and isotopic fractionation results for N in coexisting biotite and cordierite do not show any consistent behavior and, thus, factors other than temperature must be considered.

The wide range of measured N concentrations and $\delta^{15}N$ values in cordierite could be attributed to differences in the temperature of crystallization, compositional heterogeneity in the protoliths (see the compilation of data for sediments in Kerrich et al., 2006), and differing magnitudes of positive isotopic shifts in $\delta^{15}N$ resulting from lower-grade devolatilization (see Bebout and Fogel, 1992; Jia, 2006; Palya et al., 2011). Three additional effects that could explain the range of $\delta^{15}N$ values are (1) the presence of some NH_4^+ in cordierite, which could result in decreased or no fractionation of N with NH_4^+ in coexisting biotite, (2) chemical disequilibrium between biotite and cordierite that could affect the N concentrations and isotopic compositions, or (3) post-crystallization or retrograde modification of the $\delta^{15}N$ values due to differential diffusive loss (i.e., preferential loss of ^{14}N). Possibility (3) must be addressed in future studies of microporous silicates and fluid-rock processes (see discussion of diffusive loss for H_2O and CO_2 in cordierite by Vry et al., 1990). Regarding (1), we consider the presence of significant amounts

of NH_4^+ in cordierite as unlikely for crystal chemical reasons (the concentration of K, with very few exceptions, in cordierite is very low).

Nitrogen Partitioning Behavior Between Cordierite and its Rock Matrix for a Medium-Grade Schist: Nitrogen concentrations and $\delta^{15}N$ values were measured for a gem-quality cordierite and its muscovite-rich matrix for one medium-grade metasedimentary schist from Connecticut, USA (**Fig. 8b**). Here, quite interestingly, cordierite showed no measurable N within the experimental detection limits, whereas the muscovite-rich matrix contained 350 ppm N. Essentially all N in the schist resides as NH_4^+ in the micaceous matrix. This result is consistent with the observation that N concentrations in cordierite are highest at the highest metamorphic grades where muscovite is not present. The interpretation is that N residing in the muscovite, after its breakdown with increasing temperature, is taken up in K-feldspar and cordierite (see Palya et al., 2011).

Nitrogen Partitioning Behavior Between Coexisting Beryl and Muscovite

Figure 10 shows the N concentrations and $\delta^{15}N$ values for five beryl-muscovite pairs taken from four pegmatites and one metasedimentary schist (see the data in **Table 2**). These results show that muscovite always contains far greater amounts of N than coexisting beryl. A mean $\Delta^{15}N_{musc\text{-}beryl}$ ($\delta^{15}N_{musc} - \delta^{15}N_{beryl}$) value of +2.9 ($1\sigma = 1.1‰$) was obtained for these pairs. The direction and magnitude of this isotopic fractionation are similar to those measured for bioite-fluid inclusion pairs in a vein in metasedimentary rocks from Bastogne, Belgium (see discussion above) and predicted by the fractionation factors calculated using spectroscopic data (see **Fig. 2a**). Apparently, based on the limited data, the partitioning behavior of N and its isotopes between beryl and muscovite, compared to the case for cordierite-biotite pairs, is more

739 systematic (**Fig. 9**). This could, in part, reflect (1) the presence of N_2 as the single N species in
740 the beryl (i.e., not also NH_4^+) or (2) the more rapid cooling of pegmatites compared to most
741 granulites. Rapid cooling allows greater retention of N_2 incorporated during peak crystallization
742 conditions and thus better preservation of the peak-temperature partitioning behavior.
743

744 **Carbon Concentrations and $\delta^{13}C$ Values of Cordierite and Beryl**

745 **Figure 11a** shows a plot of N and C concentrations for a number of cordierites and the single
746 beryl sample studied here (see also **Table 2**). The two elements show a rough positive
747 correlation. **Figure 11b** shows a plot of C concentrations and $\delta^{13}C_{VPDB}$ values. The various
748 samples have roughly similar $\delta^{13}C$ values with a mean = -9.8‰ (1σ = 3.5‰), with the exception
749 of two cordierites outliers from granulites having $\delta^{13}C$ values of -36.4‰ and -22.3‰. For the
750 range of rocks types studied here, pegmatite cordierites tend to have lower C concentrations.
751 Cordierites from granulites and medium-grade metapelites (and the uncategorized cordierites)
752 have, in general, similar concentrations of C, but the most C-rich samples (i.e., 990 to 1200 ppm
753 C) come from granulites (there is considerable overlap among the data for medium grade,
754 granulite, and uncategorized cordierites). These observations for C concentrations and $\delta^{13}C$
755 values are consistent with those made by Vry et al. (1990) in their isotopic investigation of
756 cordierite. Beryl, unlike cordierite, contains very little C, with only one sample containing
757 amounts sufficient for an analysis of $\delta^{13}C$.
758

759 **How Important are Microporous Silicates and Tourmaline for Storage of Nitrogen in**
760 **Continental Crust?**

761 Cordierite can be a volumetrically significant rock-forming mineral in metapelitic rocks. It is
762 stable over a wide range of temperatures and at low to moderate pressures corresponding to
763 upper to middle levels of the continental crust (e.g., Schreyer, 1965; Kalt et al., 1998; White et
764 al., 2003; Palya et al., 2011). Tourmaline, which may also contain appreciable amounts of N
765 (e.g., Wunder et al., 2015), occurs in metapelitic rocks over a broader range of *P* and *T*, even in
766 UHP rocks that experienced pressures of up to ~3.0 GPa (Bebout and Nakamura, 2003; see the
767 summary by Marschall et al., 2009; van Hinsberg et al., 2011). However, its modal abundance is
768 limited in both metamorphic and igneous rocks, therefore it is unlikely to play a role as a major
769 sink in the crust and for the deep-Earth N cycle. Tourmaline and beryl in larger amounts can
770 occur in pegmatites (London and Evensen, 2002), but pegmatites are unlikely to act as
771 significant N reservoirs due to their relative scarcity. Summarizing, cordierite could be a notable
772 sink for N in shallow- to mid-levels of the continental crust.
773
774 ## CONCLUSIONS AND OUTLOOK

775 Fluxes of N among the oceanic and continental crust, mantle, oceans, and atmosphere largely
776 determine the abundance and the isotopic composition of N in all of these reservoirs. Models of
777 modern and ancient volatile cycling on Earth are highly dependent on understanding the nature
778 of these fluxes (Javoy, 1997; Tolstikihn and Marty, 1998; Zhang and Zindler, 1993). Biological
779 processes play a key role in affecting the concentrations and behavior of N in the solid Earth.
780 Nitrogen in the oceans and atmosphere can be incorporated (via biological processes) into
781 mineral phases, some of which are carried into the deep Earth (via burial and subduction).
782 Nitrogen can thus be an effective tracer in the study of the transfer of sedimentary and organic
783 components into and within the crust and upper mantle. In this article, we present some

784 important observations regarding this hydrosphere-crust-upper mantle transfer, based on the
785 studies to date, and we suggest several areas needing attention.

786 — NH_4^+ can replace K^+ via a solid solution mechanism in some K-bearing rock-forming
787 silicate minerals, especially layer silicates (clays and micas) and feldspar. This substitution is so
788 prevalent that an estimate of N subduction-input fluxes can be based on knowledge of the rates
789 of K subduction (see Busigny et al., 2003, 2011; Busigny and Bebout, 2013). Recent research
790 suggests that cordierite and tourmaline can also serve as reservoirs for N, with concentrations
791 roughly similar to those of coexisting micas. Cordierite could be a significant phase for the
792 storage of molecular N_2 in shallow- to mid-levels of the continental crust.

793 — Low-temperature devolatilization of organic matter, and the concomitant crystallization of
794 clay minerals such as illite, permit the retention of this initially-organic N as NH_4^+ in these clay
795 minerals, apparently with little isotopic fractionation. Although whole-rock C/N ratios of very
796 low-grade metamorphosed sediments can retain biogeochemical information, kerogen itself (the
797 reduced C reservoir) contains very little N. Most of the initially-organic N is transferred into and
798 housed in clays and low-grade metamorphic micas (and in some cases, authigenic feldspars;
799 Svensen et al., 2008).

800 — Considerable loss of N from minerals to fluids can occur at low to medium metamorphic
801 grades, depending upon the prograde *P-T* path the rocks experience (see Bebout and Fogel, 1992;
802 Busigny et al., 2013; Li and Keppler, 2014). In many cases, the isotopic shifts associated with
803 this loss point to a N_2-NH_4^+ exchange mechanism. Li et al. (2009) proposed, however, the
804 possibility of kinetically controlled NH_3-NH_4^+ exchange. In relatively "cool" subduction zone
805 settings, sedimentary rocks can retain a large fraction of their original N contents to great depths,
806 perhaps even the depths beneath volcanic fronts (see Busigny et al., 2003; Bebout et al., 2013a).

Experimental phase equilibrium studies document the stability of mica (e.g., phengite), the key N mineral reservoir, to great depths in most subduction zones (Schmidt and Poli, 2014).

— Further investigation of the concentrations, isotope compositions, and fluxes of N into and within the continental crust is badly needed (see the discussion by Johnson and Goldblatt, 2015). The estimated average concentration of 56 ppm for this reservoir is based on a very small number of analyses (see Wedepohl, 1995; Bach et al., 1999; Palya et al., 2011; Rudnick and Gao, 2014). It goes without saying that further work on the concentrations and isotopic compositions of N in the mantle is needed, as the mantle could contain ~60% of the Earth's N (**Table 1**; see the discussions by Cartigny and Marty, 2013; cf. Johnson and Goldblatt, 2015).

— The rates and mechanisms by which N, or its components, diffuse in key minerals such as the micas, alkali feldspars, clinopyroxenes, and microporous silicates are poorly understood (see Watson and Cherniak, 2014). Closure temperatures for the retention of N in these phases are not known, complicating the assessment of N isotope behavior at high geologic temperatures.

— All research done thus far on N in silicate systems has been on either whole-rock samples or mineral separates. It will be important to develop microanalytical methods for analyzing N concentrations and $\delta^{15}N$ at scales allowing consideration of intramineral heterogeneity (see the first analyses on cordierite using the ion microprobe by Hervig et al., 2014).

— Finally, we stress the need for experimental calibration of N isotope fractionation in silicate fluid-mineral systems. This is required to understand and resolve the differences among the various calculated fractionation factors.

ACKNOWLEDGMENTS

Funding from the National Science Foundation (most recently, EAR-0711355) supported the N isotope work conducted at Lehigh University. CAG is supported by the Austrian Science Fund

(FWF) through grant P25597-N20. We thank George Harlow and Jamie Newman, at the American Museum of Natural History (New York, NY), for assisting in the acquisition of some specimens. The cordierite samples investigated in this and the degassing study (Geiger et al., in preparation) were supplied by several colleagues and here Julie Vry (Victoria University of Wellington, New Zealand) deserves special thanks. Thanks also go to Long Li, who prepared the size splits of the beryl sample used in the tests of the release during heating. Comments by Daniele Pinti and an anonymous reviewer improved the manuscript.

REFERENCES CITED

Ader, M., Boudou, J.-P., Javoy, M., Goffe, B., and Daniels, E. (1998) Isotope study on organic nitrogen of Westphalian anthracites from the Western Middle field of Pennsylvania (U.S.A.) and from the Bramsche Massif (Germany). Organic Geochemistry, 29, 315-328.

Ader, M., Cartigny, P., Boudou, J. P., Oh, J. H., Petit, E., and Javoy, M. (2006) Nitrogen isotopic evolution of carbonaceous matter during metamorphism: Methodology and preliminary results. Chemical Geology, 232, 152-169.

Andersen, T., Austrheim, H., and Burke, E. A. J. (1990) Fluid inclusions in granulites and eclogites from the Bergen Arcs, Caledonides of Western Norway. Mineralogical Magazine, 54, 145–158.

Andersen, T., Austrheim, H., Burke, E. A., Elvevold, S. (1993) N_2 and CO_2 in deep crustal fluids: Evidence from the Caledonides of Norway. Chemical Geology, 108, 113-132.

Armbruster, T. (1985) Ar, N_2 and CO_2 in the structural cavities of cordierite, an optical and X-ray single crystal study. Physics and Chemistry of Minerals, 12, 233– 245.

Armbruster, T. (1986) Role of Na in the structure of low-cordierite: A single-crystal X-ray study. American Mineralogist, 71, 746–757.

Bach, W., Naumann, D., and Erzinger, J. (1999) A helium, argon, and nitrogen record of the upper continental crust (KTB drill holes, Oberpfalz, Germany): implications for crustal degassing. Chemical Geology, 160, 81-101.

Bakker, R. M., and Jansen, J. B. H. (1993) Calculated fluid evolution path versus fluid inclusion data in the COHN system as exemplified by metamorphic rocks from Rogaland, southwest Norway. Journal of Metamorphic Geology, 11, 357-370.

Barker, D. S. (1964) Ammonium in alkali feldspar. Am Mineral 49, 851–858.

Bebout, G. E. (1997) Nitrogen isotope tracers of high-temperature fluid-rock interactions: case study of the Catalina Schist, California. Earth and Planetary Science Letters, 151, 77-90.

Bebout, G. E. (2007) Metamorphic chemical geodynamics of subduction zones. Earth and Planetary Science Letters, 260, 373-393.

Bebout, G. E., Agard, P., Kobayashi, K., Moriguti, T., and Nakamura, E. (2013a) Devolatilization history and trace element mobility in deeply subducted sedimentary rocks: Evidence from Western Alps HP/UHP suites. Chemical Geology, 342, 1-20.

Bebout, G. E., Banerjee, N. R., Izawa, M. R., Kobayashi, K., Lazzeri, K., Ranieri, L., and Nakamura, E. (in review) Nitrogen concentrations and isotopic compositions of altered terrestrial glass basaltic rocks, and implications for astrobiology, submitted to Astrobiology.

Bebout, G. E., and Barton, M. D. (1993) Metasomatism during subduction: products and possible paths in the Catalina Schist, California. Chemical Geology, 108, 61-92.

Bebout, G. E., Cooper, D. C., Bradley, A. D., and Sadofsky, S. J. (1999a) Nitrogen-isotope record of fluid rock interactions in the Skiddaw Aureole and granite, English Lake District. American Mineralogist, 84, 1495-1505.

Bebout, G. E., and Fogel, M. L. (1992) Nitrogen-isotope compositions of metasedimentary rocks in the Catalina Schist, California - Implications for metamorphic devolatilization history. Geochimica et Cosmochimica Acta, 56, 2839-2849.

Bebout, G. E., Fogel, M. L., and Cartigny, P. (2013b) Nitrogen: Highly volatile yet surprisingly compatible. Elements, 9, 333-338.

Bebout, G. E., Idleman, B. D., Li, L., and Hilkert, A. (2007) Isotope-ratio-monitoring gas chromatography methods for high-precision isotopic analysis of nanomole quantities of silicate nitrogen. Chemical Geology, 240, 1-10.

Bebout, G. E., and Nakamura, E. (2003) Record in metamorphic tourmalines of subduction zone devolatilization and boron cycling. Geology, 31, 407-410.

Bebout, G. E., Ryan, J. G., Leeman, W. P., and Bebout, A. E. (1999b) Fractionation of trace elements by subduction-zone metamorphism – effect of convergent-margin thermal evolution. Earth and Planetary Science Letters, 171, 63-81.

Bebout, G. E., and Sadofsky, S. J., 2004, $\delta^{15}N$ analyses of ammonium-rich silicate minerals by sealed-tube extractions and dual inlet, viscous-flow mass spectrometry, in Handbook of Stable Isotope Techniques (Pier de Groot, editor), p. 348-360.

Beinlich, A., Klemd, R., John, T., and Gao, J. (2010) Trace-element mobilization during Ca-metasomatism along a major fluid conduit: Eclogitization of blueschist as a consequence of fluid-rock interaction Geochimica et Cosmochimica Acta, 74, 1892-1922.

Bertoldi, C., Proyer, A., Garbe-Schonberg, D., Behrens, H., and Dachs, E. (2004) Comprehensive chemical analyses of natural cordierites: implications for exchange mechanisms. Lithos, 78, 389-409.

Bobos, I., and Eberl, D. D. (2013) Thickness distributions and evolution of growth mechanisms of NH_4-illite from the fossil hydrothermal system of Harghita Bãi, Eastern Carpathians, Romania. Clays and Clay Minerals, 61, 375-391.

Bos A., Duit W., van Der Eerden M. J., and Jansen B. (1988) Nitrogen storage in biotite: An experimental study of the ammonium and potassium partitioning between 1 M-phlogopite and vapour at 2 kb. Geochimica et Cosmochimica Acta, 52, 1275–1283.

Bottrell, S. H., Carr, L. P., and Dubessy, J. (1988) A nitrogen-rich metamorphic fluid and coexisting minerals in slates from North Wales. Mineralogical Magazine, 52, 451-457.

Boudou, J.-P., Schimmelmann, A., Ader, M., Mastalerz, M., Sebilo, M., and Gengembre, L. (2008) Organic nitrogen chemistry during low-grade metamorphism. Geochimica et Cosmochimica Acta, 72, 1199-1221.

Boyd, S. R. (1997) Determination of the ammonium content of potassic rocks by capacitance manometry: a prelude to the calibration of FTIR microscopes. Chemical Geology, 137, 57-66.

Boyd, S. R. (2001) Nitrogen in future biosphere studies. Chemical Geology, 176, 1-30.

Boyd, S. R., Hall, A., and Pillinger, C. T. (1993) The measurement of $\delta^{15}N$ in crustal rocks by static vacuum mass spectrometry: Application to the origin of the ammonium in the Cornubian batholith, southwest England. Geochimica et Cosmochimica Acta, 57, 1339-1347.

Bräuer, K., and Hahne, K. (2005) Methodical aspects of the ^{15}N-analysis of Precambrian and Palaeozoic sediments rich in organic matter. Chemical Geology, 218, 361-368.

Bul'bak, T. A., and Shvedenkov, G. Y. (2005) Experimental study on incorporation of C-H-O-N fluid components in Mg-cordierite. European Journal of Mineralogy, 17, 829-838.

Busigny, V., Ader, M., and Cartigny, P. (2005a) Quantification and isotopic analysis of nitrogen in rocks at the ppm level using tube combustion technique: A prelude to the study of altered oceanic crust. Chemical Geology, 223, 249–258.

Busigny, V., and Bebout, G. E. (2013) Nitrogen in the silicate Earth: Speciation and isotopic behavior during mineral–fluid interactions. Elements, 9, 353-358.

Busigny, V., Cartigny, P., and Philippot, P. (2011) Nitrogen isotopes in ophiolitic metagabbros: A reevaluation of modern nitrogen fluxes in subduction zones and implication for the early Earth atmosphere. Geochimica et Cosmochimica Acta, 75, 7502-7521.

Busigny, V., Cartigny, P., Philippot, P., Ader, M., and Javoy, M. (2003) Massive recycling of nitrogen and other fluid-mobile elements (K, Rb, Cs, H) in a cold slab environment: evidence from HP to UHP oceanic metasediments of the Schistes Lustres nappe (western Alps, Europe). Earth and Planetary Science Letters, 215, 27-42.

Busigny, V., Cartigny, P., Philippot, P., and Javoy, M. (2004) Quantitative analysis of ammonium in biotite using infrared spectroscopy. American Mineralogist, 89, 1625-1630.

Busigny, V., Laverne, C., and Bonifacie, M. (2005b) Nitrogen content and isotopic composition of oceanic crust at a superfast spreading ridge: A profile in altered basalts from ODP Site 1256, Leg 206. Geochemistry Geophysics Geosystems, 6, doi:10.1029/2005GC001020.

Cartigny, P. (2005) Stable isotopes and the origin of diamond. Elements, 1, 79-84.

Cartigny, P., Busigny, V., and Rudnick, R. (2013) Re-investigating the nitrogen budget in the upper continental crust. Goldschmidt Conference abstracts, p. 835.

Cartigny, P., De Corte, K., Shatsky, V. S., Ader, M., De Paepe, P., Sobolev, N. V., and Javoy, M. (2001) The origin and formation of metamorphic microdiamonds from the Kokchetav massif, Kazakhstan: a nitrogen and carbon isotopic study. Chemical Geology, 176, 265-281.

Cartigny, P., and Marty, B. (2013) Nitrogen isotopes and mantle geodynamics: The emergence of life and the atmosphere-crust-mantle connection. Elements, 9, 359-366.

Clarke, D. B. (1995) Cordierite in felsic igneous rocks: A synthesis. Mineralogical Magazine, 59, 311-325.

Cockell, C. S., van Calsteren, P., Mosselmans, J. F. W., Franchi, I. A., Gilmour, I., Kelly, L., Olsson-Francis, K., Johnson, D., and the JC24 Shipboard scientific party (2010) Microbial endolithic colonization and the geochemical environment in young seafloor basalts. Chemical Geology, 279, 17-30.

Collins, N. C., Bebout, G. E., Angiboust, S., Agard, P., Scambelluri, M., Crispini, L., John, T. (in press) Subduction zone metamorphic pathway for deep carbon cycling: II. Evidence from HP/UHP metabasaltic rocks and ophicarbonates. Chemical Geology.

Cook-Kollars, J., Bebout, G. E., Collins, N. C., Angiboust, S., and Agard, P. (2014) Subduction zone metamorphic pathway for deep carbon cycling: I. Evidence from HP/UHP metasedimentary rocks,

Italian Alps. Chemical Geology, 386, 31-48.

Damon, P. E., and Kulp, J. L. (1958) Excess helium and argon in beryl and other minerals. American Mineralogist, 43, 433-459.

Darimont, A., Burke, E., and Touret, J. (1988) Nitrogen-rich metamorphic fluids in Devonian metasediments from Bastogne, Belgium. Bulletin Mineralogie, 111, 321-330.

Dobrzhinetskaya, L. F., Wirth, R., Yang, J., Hutcheon, I. D., Weber, P. K., and Green, H. W. (2009) High pressure highly reduced nitrides and oxides from chromitite of a Tibetan ophiolite. Proceedings of the National Academy of Sciences, 106, 19233–19238.

Duit, W., Jansen, J. B. H., van Breeman, A., and Bos, A. (1986) Ammonium micas in metamorphic rocks as exemplified by Dome de L'Agout (France). American Journal of Science, 286, 702-732.

Elkins, L. J., Fischer, T. P., Hilton, D. R., Sharp, Z. D., McKnight, S., and Walker, J. (2006) Tracing nitrogen in volcanic and geothermal volatiles from the Nicaraguan volcanic front. Geochimica et Cosmochimica Acta, 70, 5215-5235.

Erd, R. C., White, D. E., Fahey, J. J., and Lee, D. E. (1964) Buddingtonite, an ammonium feldspar with zeolitic water. American Mineralogist, 49, 831-850.

Eugster, H. P., and Munoz, J. (1966) Ammonium micas: possible sources of atmospheric ammonia and nitrogen. Science, 151, 683-686.

Facq, S., Daniel, I., Montagnac, G., Cardon, H., and Sverjensky, D. A. (2014) *In situ* Raman study and thermodynamic model of aqueous carbonate speciation in equilibrium with aragonite under subduction zone conditions. Geochimica et Cosmochimica Acta, 132, 375-390.

Fischer, T. (2008) Fluxes of volatiles (H_2O, CO_2, N_2, Cl, F) from arc volcanoes. Geochemical Journal, 42, 21-38.

Galloway, J. N. (2003) 8.12. The global nitrogen cycle. Treatise on Geochemistry, Elsevier, 557-583.

Geiger, C. A., Rahmoun, N.-S., and Heide, K. (in preparation) Cordierite V: A high-temperature microporous silicate with occluded molecular species.

Goldblatt, C., Claire, M. W., Lenton, T. M., Matthews, A. J., Watson, A. J., and Zahnle, K. J. (2009) Nitrogen enhanced greenhouse warming on early Earth. Nature Geoscience, 2, 891-896.

Grove, M., and Bebout, G. E. (1995) Cretaceous tectonic evolution of coastal southern California: insights from the Catalina Schist. Tectonics, 14, 1290-1308.

Haendel, D., Mühle, K., Nitzsche, H., Stiehl, G., and Wand, U. (1986) Isotopic variations of the fixed nitrogen in metamorphic rocks. Geochimica et Cosmochimica Acta, 50, 749-758.

Halama, R., Bebout, G. E., John, T., and Marschall, H. (in review) Evidence for subduction-zone mobility of nitrogen in lithological traverses of HP/UHP-metamorphosed sedimentary, basaltic, and ultramafic rocks. Earth and Planetary Science Letters.

Halama, R., Bebout, G. E., John, T., and Scambelluri, M. (2012) Nitrogen recycling in subducted mantle rocks and implications for the global nitrogen cycle. International Journal of Earth Sciences, doi:10.1007/s00531-012-0782-3.

Halama, R., Bebout, G. E., John, T., and Schenk, V. (2010) Nitrogen recycling in subducted oceanic lithosphere: the record in high- and ultrahigh-pressure metabasaltic rocks. Geochimica et Cosmochimica Acta, 74, 1636-1652.

Hall, A. (1999) Ammonium in granites and its petrogenetic significance. Earth-Science Reviews, 45, 145-165.

997 Hall, A., Pereira, M. D., and Bea, F. (1996) The abundance of ammonium in the granites of central Spain,
998 and the behaviour of the ammonium ion during anatexis and fractional crystallization. Mineralogy
999 and Petrology, 56, 105-123.

1000 Hashizume, K., and Marty, B. (2005) Nitrogen isotopic analyses at the sub-picomole level using an ultra-
1001 low blank laser extraction technique, in: de Groot, P. (Ed.), Handbook of stable isotope analytical
1002 techniques. Elsevier, Amsterdam.

1003 Hanschmann, G. (1981) Berechnung von isotopieeffekten auf quantenchmischer grundlage am beispiel
1004 stickstoff fhaltiger moleküle. ZFI-Mitteilungen, 41, 19-39.

1005 Heinrich, E. W. (1950) Cordierite in pegmatite near Micanite, Colorado. Americal Mineralogist, 35, 173-
1006 184.

1007 Hervig, R. L., Fudge, C., and Navrotsky, A. (2014) Analyzing nitrogen in cordierites and other phases by
1008 SIMS. Goldschmidt Conference abstract 982.

1009 Higashi, S. (1982) Tobelite, a new ammonium dioctahedral mica. Mineralogical Journal, 11, 138-146.

1010 Hilton, D. R., Fischer, T. P., and Marty, B. (2002) Noble gases and volatile recycling at subduction zones.
1011 Reviews in Mineralogy and Geochemistry, 47, 319-370.

1012 Holloway, J. M., and Dahlgren, R. A. (2002) Nitrogen in rock: Occurrences and biogeochemical
1013 implications. Global Biogeochemical Cycles, 16, doi:10.1029/2002GB001862.

1014 Honma, H., and Itihara, Y. (1981) Distribution of ammonium in minerals of metamorphic and granitic
1015 rocks. Geochimica et Cosmochimica Acta, 45, 983-988.

1016 Javoy, M. (1997) The major volatile elements of the Earth: their origin, behavior, and fate. Geophysical
1017 Research Letters, 24, 177-180.

1018 Jenden, P. D., Kaplan, I. R., Poreda, R. J., and Craig, H. (1988) Origin of nitrogen-rich natural gases in
1019 the California Great Valley: Evidence from helium, carbon, and nitrogen isotope ratios. Geochimica
1020 et Cosmochimica Acta, 52, 85l-861.

1021 Jia, Y. F. (2006) Nitrogen isotope fractionations during progressive metamorphism: A case study from the
1022 Paleozoic Cooma metasedimentary complex, southeastern Australia. Geochimica et Cosmochimica
1023 Acta, 70, 5201-5214.

1024 Jia, Y., Kerrich, R., and Goldfarb, R. (2003) Metamorphic origin of ore-forming fluids for orogenic gold-
1025 bearing quartz vein systems in the North American Cordillera: Constraints from a reconnaissance
1026 study of $\delta^{15}N$, δD, and $\delta^{18}O$. Economic Geology, 98, 109-123.

1027 John, T., Gussone, N., Podladchikov, Y. Y., Bebout, G. E., Dohmen, R., Halama, R., Klemd, R., Magna,
1028 T., and Seitz, M. (2012) Pulsed long-distance fluid flow through subducting slabs feeds volcanic arcs.
1029 Nature Geoscience, doi: 10.1038/NGEO1482.

1030 Johnson, B., and Goldblatt, C. (2015) The nitrogen budget of Earth, Earth Science Reviews, doi:
1031 10.1016/j.earscirev.2015.05.006

1032 Junge, F., Seltmann, R., and Stiehl, G. (1989) Nitrogen isotope characteristics of breccias, granitoids, and
1033 greisens from eastern Erzgebirge tin ore deposits (Sadisdorf: Altenberg), GDR. Proc. 5th Working
1034 Mtg., Isotopes in Nature, Leipzig, September, l989, pp. 321-332.

1035 Kalt, A., Altherr, R., and Ludwig, T. (1998) Contact metamorphism in pelitic rocks on the island of Kos
1036 (Greece, Eastern Aegean Sea): a Test for the Na-in-cordierite thermometer. Journal of Petrology, 39,
1037 663-688.

1038 Kerrich, R., Jia, Y., Manikyamba, C., and Naqvi, S. M. (2006) Secular variations of N-isotopes in
1039 terrestrial reservoirs and ore deposits. in S. E. Kesler and H. Ohmoto (Editors), Evolution of Early

1040 Earth's Atmosphere, Hydrosphere, and Biosphere—Constraints from Ore Deposits. Geological
1041 Society of America Memoir, 198, 81–104.

1042 Kolesov, B. A., and Geiger, C. A. (2000) Cordierite II: The role of CO_2 and H_2O. American Mineralogist,
1043 85, 1265-1274.

1044 Kreulen, R., and Schuiling, R. D. (1982) N_2-CH_4-CO_2 fluids during formation of the Dome de l'Agout,
1045 France. Geochimica et Cosmochimica Acta, 46, 193-203.

1046 Kreulen, R., van Breeman, A., and Duit, W. (1982) Nitrogen and carbon isotopes in metamorphic fluids
1047 from the Dome de L'Agout, France. Proceedings of the 5th International Conference for
1048 Geochronology, Cosmochronology, and Isotope Geology, p. 191.

1049 Krohn, M. D., Kendall, C., Evans, J. R., and Fries, T. L. (1993) Relations of ammonium minerals at
1050 several hydrothermal systems in the western U.S. Journal of Volcanology and Geothermal Research,
1051 4, 401-413.

1052 Krooss, B. M., Friberg, L., Gensterblum, Y., Hollenstein, J., Prinz, D., and Littke, R. (2005) Investigation
1053 of the pyrolytic liberation of molecular nitrogen form Paleeozoic sedimentary rocks. International
1054 Journal of Earth Sciences, 94, 1023-1038.

1055 Lazzeri, K. E. (2012) Storage of Nitrogen in Silicate Minerals and Glasses. M.S. thesis, Lehigh
1056 University, 76 pp.

1057 Lepezin, G. G., Bul'bak, T. A., Sokol, E. V., and Shvedenkov, G. Yu. (1999) Fluid components in
1058 cordierites and their significance for metamorphic petrology. Russian Geology and Geophysics, 40,
1059 99-116.

1060 Li, L., Bebout, G. E., and Idleman, B. D. (2007) Nitrogen concentration and $\delta^{15}N$ of altered oceanic crust
1061 obtained on ODP Legs 129 and 185: Insights into alteration-related nitrogen enrichment and the
1062 nitrogen subduction budget. Geochimica et Cosmochimica Acta, 71, 2344-2360.

1063 Li, L., Cartigny, P., and Ader, M. (2009) Kinetic nitrogen isotope fractionation associated with thermal
1064 decomposition of NH_3: Experimental results and potential applications to trace the origin of N_2 in
1065 natural gas and hydrothermal systems. Geochimica et Cosmochimica Acta, 73, 6282-6297.

1066 Li, L., Zheng, Y.-F., Cartigny, P., and Li, J. (2014) Anomalous nitrogen isotopes in ultrahigh-pressure
1067 metamorphic rocks from the Sulu orogenic belt: Effect of abiotic nitrogen reduction during fluid-rock
1068 interaction. Earth and Planetary Science Letters, 403, 67-78.

1069 Li, Y., and Keppler, H. (2014) Nitrogen speciation in mantle and crustal fluids. Geochimica et
1070 Cosmochimica Acta, 129, 13-32.

1071 Libourel, G., Marty, B., and Humbert, F. (2003) Nitrogen solubility in basaltic melt. Part I. Effect of
1072 oxygen fugacity. Geochimica et Cosmochimica Acta, 67, 4123-4135.

1073 London, D., and Evensen, J. M. (2002) Beryllium in silicic magmas and the origin of beryl-bearing
1074 pegmatites. Reviews in Mineralogy and Geochemistry, 50, 445-486.

1075 Mariotti, A. (1984) Natural ^{15}N abundance measurements and atmospheric nitrogen standard calibration.
1076 Nature, 311, 251-252.

1077 Marschall, H. R., Korsakov, A. V., Luvizotto, G. L., Nasdala, L., and Ludwig, T. (2009) On the
1078 occurrence and boron isotopic composition of tourmaline in (ultra)high-pressure metamorphic rocks.
1079 Journal of the Geological Society, London, 177, 811-823.

1080 Mashkovtsev, R. I., and Solntsev, V. P. (2002) Channel constituents in synthetic beryl: ammonium.
1081 Physics and Chemistry of Minerals, 29, 65-71.

1082 Mikhail, S., and Sverjensky, D. A. (2014) Nitrogen speciation in upper mantle fluids and the origin of

Earth's nitrogen-rich atmosphere. Nature Geoscience, 7, doi:10.1038/NGEO2271.

Mingram, B., and Bräuer, K. (2001) Ammonium concentration and nitrogen isotope composition in metasedimentary rocks from different tectonometamorphic units of the European Variscan Belt. Geochimica et Cosmochimica Acta, 65, 273-287.

Mingram, B., Hoth, P., Luders, V., and Harlov, D. (2005) The significance of fixed ammonium in Palaeozoic sediments for the generation of nitrogen-rich natural gases in the North German Basin. International Journal of Earth Sciences, 94, 1010-1022.

Mitchell, E. C., Fischer, T. P., Hilton, D. R., Hauri, E. H., Shaw, A. M., de Moor, J. M., Sharp, Z. D., and Kazahaya, K. (2010) Nitrogen sources and recycling at subduction zones: insights from the Izu–Bonin–Mariana arc. Geochemistry, Geophysics, Geosystems, 11(2), doi.org/10.1029/2009GC002783.

Moine, B., Guillot, C., and Gibert, F. (1994) Controls on the composition of nitrogen-rich fluids originating from reaction with graphite and ammonium-bearing biotite. Geochimica et Cosmochimica Acta, 58, 5503-5523.

Müller, E. P., May, F., and Stiehl, G. (1976) Zur Isotopengeochemie des Stickstoffs und zur Genese stickstoffreicher Erdgase. Zeitschrift für Angewandte Geologie, 22, 319–324.

Mysen, B., and Fogel, M. L. (2010). Nitrogen and hydrogen isotope compositions and solubility in silicate melts in equilibrium with reduced (N+H)-bearing fluids at high pressure and temperature: Effects of melt structure. American Mineralogist, 95, 987-999.

Ortega, L., Vendel, E., and Beny, C. (1991) C-O-H-N fluid inclusions associated with gold-stibnite mineralization in low-grade metamorphic rocks, Mari Rosa mine, Caceras, Spain. Mineralogical Magazine, 55, 235-247.

Palya, A. P., Buick, I. S., and Bebout, G. E. (2011) Storage and mobility of nitrogen in the continental crust: Evidence from partially melted metasedimentary rocks, Mt. Stafford, Australia. Chemical Geology, 281, 211-226.

Pan, D., Spanu, L., Harrison, B., Sverjensky, D. A., and Galli, G. (2013) Dielectric properties of water under extreme conditions and transport of carbonates in the deep Earth. Proceedings of the National Academy of Sciences, 110, 6646-6650.

Philippot, P., Busigny, V., Scambelluri, M., and Cartigny, P. (2007) Oxygen and nitrogen isotopes as tracers of fluid activities in serpentinites and metasediments during subduction. Mineralogy and Petrology, 91, 11-24.

Pinti, D. L., Hashizume, K., Orberger, B., Gallien, J.-P., Cloquet, C., and Massault, M. (2007) Biogenic nitrogen and carbon in Fe-Mn-oxyhydroxides from an Archean chert, Marble Bar, Western Australia. Geochemistry, Geophysics, and Geosystems, 8, doi:10.1029/2006GC001394.

Pitcairn, I. K., Teagle, D. A. H., Kerrich, R., Craw, D., and Brewer, T. S. (2005) The behavior of nitrogen and nitrogen isotopes during metamorphism and mineralization: Evidence from the Otago and Alpine Schists, New Zealand. Earth and Planetary Science Letters, 233, 229-246.

Plessen, B., Harlov, D. E., Henry, D., and Guidotti, C. V. (2010) Ammonium loss and nitrogen isotopic fractionation in biotite as a function of metamorphic grade in metapelites from western Maine, USA. Geochimica et Cosmochimica Acta, 74, 4759-4771.

Pöter, B., Gottschalk, M., and Heinrich, W. (2004) Experimental determination of the ammonium partitioning among muscovite, K-feldspar, and aqueous chloride solutions. Lithos, 74, 67-90.

Richet, P., Bottinga, Y., and Javoy, M. (1977) A review of hydrogen, carbon, nitrogen, oxygen, sulphur and chlorine stable isotope fractionation among gaseous molecules. Annual Review of Earth and Planetary Sciences, 5, 65-110.

Roskosz, M., Bouhifd, M., Jephcoat, A., Marty, B., and Mysen, B. (2013) Nitrogen solubility in molten metal and silicate at high pressure and temperature. Geochimica et Cosmochimica Acta, 121, 15–28.

Roskosz, M., Mysen, B., and Cody, G. D. (2006) Dual speciation of nitrogen in silicate melts at high pressure and temperature: An experimental study. Geochimica et Cosmochimica Acta, 70, 2902-2918.

Rudnick, R. L., and Gao, A. (2014) 4.1 Composition of the continental crust. In: Holland, H.D., Turekian, K.K. (Eds.), Treatise on Geochemistry, 4. Elsevier, Amsterdam, pp. 1–51.

Ruiz Cruz, M. D., and Sanz de Galdeano, C. (2008) High-temperature ammonium white mica from the Betic Cordillera (Spain). American Mineralogist, 93, 977-987.

Sadofsky, S. J., and Bebout, G. E. (2000) Ammonium partitioning and nitrogen-isotope fractionation among coexisting micas during high-temperature fluid-rock interactions: examples from the New England Appalachians. Geochimica et Cosmochimica Acta, 64, 2835-2849.

Sadofsky, S. J., and Bebout, G. E. (2003) Record of forearc devolatilization in low-T, high-P/T metasedimentary suites: significance for models of convergent margin chemical cycling, Geochemistry, Geophysics, and Geosystems, doi:10.1029/2002GC000412.

Sadofsky, S. J., and Bebout, G. E. (2004) Nitrogen geochemistry of subducting sediments: new results from the Izu-Bonin-Mariana margin and insights regarding global N subduction. Geochemistry, Geophysics, and Geosystems, doi:10.1029/2003GC000543.

Sano, Y., Takahata, N., Nishio, Y., Fischer, T. P., and Williams, S. N. (2001) Volcanic flux of nitrogen from the Earth. Chemical Geology, 171, 263-271.

Scalan, R. S. (1958) The isotopic composition, concentration, and chemical state of the nitrogen in igneous rocks. Ph.D. dissertation, University of Arkansas.

Schmidt, M. W., and Poli, S. (2014) Devolatilization during subduction, in Rudnick, R. L., ed., 2nd Ed. Volume 3, Treatise on Geochemistry: The Crust, Elsevier, pp. 669-701.

Schreyer, W. (1965) Synthetische und natürliche Cordierit II. Die chemischen Zusammensetzung natürlicher Cordierite und ihre Abhängigkeit von den PTX-Bedingungen bei der Gesteinsbildung. Neues Jahrbuch für Mineralogie - Abhandlung,103, 35-79.

Schroeder, P. A., and McLain, A. A. (1998) Illite-smectites and the influence of burial diagenesis on the geochemical cycling of nitrogen. Clay Minerals, 33, 539-546.

Staudigel, H., Furnes, H., McLoughlin, N., Banerjee, N. R., Connell, L. B., and Templeton, A. (2008) 3.5 billions years of glass bioalteration: Volcanic rocks as a basis for microbial life? Earth-Science Reviews, 89, 156-176.

Svensen, H., Bebout, G. E., Kronz, A., Li, L., Planke, S., Chevallier, L., and Jamtveit, B. (2008) Nitrogen geochemistry as a tracer of fluid flow in a hydrothermal vent complex in the Karoo Basin, South Africa. Geochimica et Cosmochimica Acta, 72, 4929-4947.

Sverjensky, D. A., Stagno, V., and Huang, F. (2014) Important role for organic carbon in subduction-zone fluids in the deep carbon cycle. Nature Geoscience, 7, 909-913.

Thomazo, C., Ader, M., and Philippot, P. (2011) Extreme ^{15}N-enrichments in 2.72-Gyr-old sediments: Evidence for a turning point in the nitrogen cycle. Geobiology, 9, 107-120.

Thomazo, C., and Papineau, D. (2013) Biogeochemical cycling of nitrogen on the early Earth. Elements, 9, 345-352.

Tolstikihn, I. N., and Marty, B. (1998) The evolution of terrestrial volatiles: a view from helium, neon, argon and nitrogen isotope modeling. Chemical Geology, 147, 27-52.

Touret, J. L. R. (2001) Fluids in metamorphic rocks. Lithos, 55, 1-25.

van Hinsberg, V. J., Henry, D. J., and Dutrow, B. L. (2011) Tourmaline as a petrologic forensic mineral: A unique recorder of its geologic past. Elements, 7, 327-332.

Vernon, R. H., Clarke, G. L., and Collins, W. J. (1990) Local, mid-crustal granulite facies metamorphism and melting: an example in the Mt. Stafford area, central Australia. in: Ashworth, J.R., Brown, M. (Eds.), High Temperature Metamorphism and Crustal Anatexis. Unwin Hyman, London, pp. 272–319.

Visser, D. (1992) On ammonium in upper-amphibolite facies cordierite-orthoamphibole-bearing rocks from Rod, Bamble Sector, south Norway. Norsk Geologisk Tiddskrift, 72, 385-388.

Vry, K. J., Brown, P. E., and Valley, J. W. (1990) Cordierite volatile content and the role of CO_2 in high grade metamorphism. American Mineralogist, 75, 71-88.

Watenphul, A., Wunder, B., Wirth, R., and Heinrich, W. (2010) Ammonium-bearing clinopyroxene: A potential nitrogen reservoir in the Earth's mantle. Chemical Geology, 270, 240-248.

Watson, E. B., and Cherniak, D. J. (2014) Diffusion and solubility of nitrogen in olivine. Goldschmidt Conference abstract 2664.

Wedepohl, H. (1995) The composition of the continental crust. Geochimica et Cosmochimica Acta, 59, 1217–1239.

White, R. W., Powell, R., and Clarke, G. I. (2003) Prograde metamorphic assemblage evolution during partial melting of metasedimentary rocks at low pressures: migmatites from Mt. Stafford, Central Australia. Journal of Petrology, 44, 1937-1960.

Williams, L. B., Ferrell Jr., R. E., Chinn, E. W., and Sassen, R. (1989) Fixed-ammonium in clays associated with crude oils. Applied Geochemistry, 4, 605-616.

Williams, L. B., Ferrell Jr., R. E., Hutcheon, I., Bakel, A. J., Walsh, M. M., and Krouse, H. R. (1995) Nitrogen isotope geochemistry of organic matter and minerals during diagenesis and hydrocarbon migration. Geochimica et Cosmochimica Acta, 59, 765-779.

Wlotzka, F., 1972. Handbook of Geochemistry. volume II. Springer-Verlag.

Wunder, B., Berryman, E., Plessen, B., Rhede, D., Koch-Müller, M., and Heinrich, W. (2015) Synthetic and natural ammonium-bearing tourmaline. American Mineralogist, 100, 250-256.

Yokochi, R., Marty, B., Chazot, G., and Burnard, P. (2009) Nitrogen in peridotite xenoliths: Lithophile behavior and magmatic isotope fractionation. Geochimica et Cosmochimica Acta, 73, 4843-4861.

Zhang, Y., and Zindler, A. (1993) Distribution and evolution of carbon and nitrogen in Earth. Earth and Planetary Science Letters, 117, 331–345.

FIGURE CAPTIONS

Figure 1. Flow-chart diagram illustrating the various N reservoirs on Earth and their interactions. Note especially those processes for the solid Earth involving the deposition, diagenesis, metamorphism, and melting of sediments, because they can carry surface N to deeper geologic levels (from Bebout et al., 2013b; modified after Boyd, 2001; also see Holloway and Dahlgren, 2002). W = weathering and E = erosion. The inset photograph shows a beryl–muscovite intergrowth that could contain organic-derived N as N_2 and NH_4^+ in beryl and muscovite, respectively (Lazzeri, 2012; Busigny and Bebout, 2013; see **Fig. 10**). The photograph of the beryl+muscovite sample is courtesy of Desert Winds Gems and Minerals (WWW.DESERTWINDSGEMSANDMINERALS.COM).

Figure 2. Nitrogen isotope fractionations and consequences for the evolution in the N isotope compositions of devolatilizing rocks. (**A**) Fractionation factors among N_2, NH_3, and NH_4^+. NH_4^+ is typically bound in silicates such as clays, micas, and feldspars through substitution of K^+ (from Busigny and Bebout, 2013). (**B**) Rayleigh (curves) and batch (straight lines) distillation behavior for N_2-NH_4^+ exchange at 300 and 600°C, labeled by N_2-NH_4^+ $10^3 \ln\alpha$ (modified after Svensen et al., 2008).

Figure 3. Schematic ocean-continent subduction zone (modified after Cook-Kollars et al., 2014), showing key subducted lithologies. Shown are global-basis N fluxes in g/year for the subduction of sediment, oceanic crust, and hydrated mantle, and the estimate of Hilton et al. (2002) for the return of N (in g/year) to the atmosphere via arc volcanic degassing. Fischer (2008) estimated a much larger arc volcanic output of 9×10^{11} g/yr. Subduction zone cycling of N encompasses a number of pathways discussed in this paper, i.e., low-temperature/surface incorporation into organic matter and geologic glasses, diagenetic alteration, low- to high-grade metamorphic devolatilization, and partial melting. The upper mantle is believed do have $\delta^{15}N$ values around -5‰. Subduction delivers sediment, altered oceanic crust, and hydrated ultramafic rocks, all with higher, often positive $\delta^{15}N$ values influenced by surface/near-surface organic/sedimentary processes (see Busigny et al., 2005a,b; Li et al., 2007; Halama et al., 2012; Bebout et al., 2013b, in review).

Figure 4. Whole-rock N concentrations and isotope compositions of the Schistes Lustres-Cignana and the Catalina Schist metasedimentary suites that demonstrate N retention to great depths for these rocks for their respective prograde *P-T* paths. (**A**) Whole-rock $\delta^{15}N$ values of subduction-zone-metamorphosed metapelitic-metapsammitic rocks of the W. Alps, namely the Schistes Lustres/Lago di Cignana suite exposed in NW Italy (figure from Bebout et al., 2013a). The dataset from Busigny et al. (2003) includes results for rocks believed to be the protoliths of the Schistes Lustres-Cignana suite ("Lavagna" and "Lago Nero"). The data for the lower-grade units, in general, are similar to those of the same units determined in the earlier study; however, the $\delta^{15}N$ values for the Cignana samples presented by Bebout et al. (2013a) fall at the high end of the previously published range, perhaps reflecting some N isotopic shift resulting from the minor devolatilization that these samples experienced. Numbers in brackets (blue type) indicate atomic-basis C/N ratios. (**B**) Whole-rock N and K_2O concentrations (Busigny et al. (2003; Bebout et al., 2013a) showing a positive correlation between N and K that is largely independent of metamorphic grade. The square boxes are for three samples from Lago di Cignana and the diamond-shaped box indicates one analysis of a Finestre sample from Bebout et al. (2013a). The thin gray lines parallel to the linear regression line for the Busigny data (R=0.971) indicate the limits of the envelope for the data from Busigny et al. (2003). (**C**) Whole-rock ratios of N, Cs, and B to K_2O as a function of metamorphic grade for metasedimentary rocks of the Catalina Schist (from Bebout et al., 1999b; LA = lawsonite-albite; LBS = lawsonite blueschist; EBS = epidote blueschist; EA = epidote amphibolite; AM = amphibolite). The mean value ($\pm 1\sigma$) of $\delta^{15}N$ at each grade is also indicated. (**D**) Pressure-temperature diagram showing the estimated *P-T* paths of the tectonometamorphic units for which data are presented in **C** (figure is from Grove and Bebout, 1995).

Figure 5. Behavior of N and K_2O in metasomatized blueschist-facies metaconglomerate cobbles (data from Bebout, 1997). Inset photomicrograph shows the replacement of igneous hornblende by blue (sodic) amphibole and the nearly complete replacement of now-relict plagioclase by fine-grained phengite. Error bars for N ppm are ±5% error. Errors for the measurements of K_2O are smaller than the symbol sizes.

Figure 6. Nitrogen and other trace element behavior across a vein envelope in the Tianshan investigated by Beinlich et al. (2010; N data are from Halama et al., in review). (**A**) Various trace element and $\delta^{15}N$ variation across the envelope (indicated as distance to the vein, the latter at 0 cm; see **D**); (**B**) and (**C**) Concentrations of N vs. those of K and Ba, respectively. There is a positive linear correlation in both cases; (**D**) Sketch illustrating the sampling profile and localities for the vein envelope showing a prograde blueschist-eclogite transition (JTS sequence; Beinlich et al., 2010).

Figure 7. Nitrogen behavior for the Mt. Stafford migmatite suite, Australia (all figures from Palya et al., 2011). (**A**) N/Al_2O_3, Cs/Al_2O_3, Ba/Al_2O_3, and Rb/Al_2O_3 as a function of increasing metamorphic grade (to the right side of the diagram; see the discussion in the text). (**B**) Nitrogen concentrations and $\delta^{15}N$ values of whole-rock samples. The curved lines represent calculated Rayleigh loss for various fluid/melt-NH_4^+ $10^3 \ln\alpha$ values (from Hanschmann, 1981) corresponding to N_2 or NH_3 speciation in fluids/melts and over a range of temperatures (for both fluid species, labeled on the right side of the plot, temperatures for the calculations were 327˚, 527˚, and 727˚C, from top to bottom for each species). (**C**) Outcrop photograph (camera lens cap for scale) for a typical Zone 4 Mt. Stafford exposure, where the dark layers are metapsammitic layers within lighter metapelitic layers.

Figure 8. Nitrogen concentrations and isotopic compositions of various beryl and cordierite samples. (**A**) Data for cordierite from various petrologic environments (**Table 2** and **Appendices A and B**; Lazzeri, 2012) and from the Mt. Stafford migmatites (Palya et al. (2011). The photomicrograph (horizontal dimension ~ 5 mm) is of a cordierite crystal in a Zone 4 Mt. Stafford sample containing sillimanite inclusions and within a K-feldspar-rich matrix containing no muscovite or biotite. Note that the granulitic cordierites tend to contain larger amounts of N and possibly have lower $\delta^{15}N$ values. (**B**) Photomicrograph showing inclusion-free gem-like cordierite and matrix muscovite in a medium-grade metapelitic rock from Connecticut, USA (horizontal length ~1 cm). The cordierite is N-free but the muscovite-rich matrix contains ~350 ppm N.

Figure 9. Nitrogen isotopic compositions and concentrations for coexisting cordierite and biotite pairs from different petrologic environments (**Table 2** and **Appendices A and B**; Lazzeri, 2012). The inset shows the crystal structure of microporous cordierite, green = magnesium

atoms, blue = oxygen atoms, yellow = silicon atoms, and brown or gray = aluminum atoms. Note the infinite channelways, formed by the Si/AlO_4 tetrahedra in rings, which run parallel to the *c*-axis. N_2 and other molecules occur in these channelways.

Figure 10. Nitrogen isotopic compositions and concentrations of coexisting beryl and muscovite from pegmatites and metamorphic schist (**Table 2** and **Appendix A**; Lazzeri, 2012). The inset photograph of beryl in muscovite is from minddat.org (horizontal dimension ~8 cm).

Figure 11. Carbon and N concentrations and $\delta^{13}C$ values for the cordierites and beryl analyzed in this study. (**A**) Nitrogen vs. C concentrations. Cordierites from the granulite facies tend to show the highest N concentrations and those from pegmatites the lowest, as is also the case for beryl. (**B**) Carbon concentration vs. $\delta^{13}C$ showing the relatively narrow range of isotopic compositions and the wide range in C concentrations.

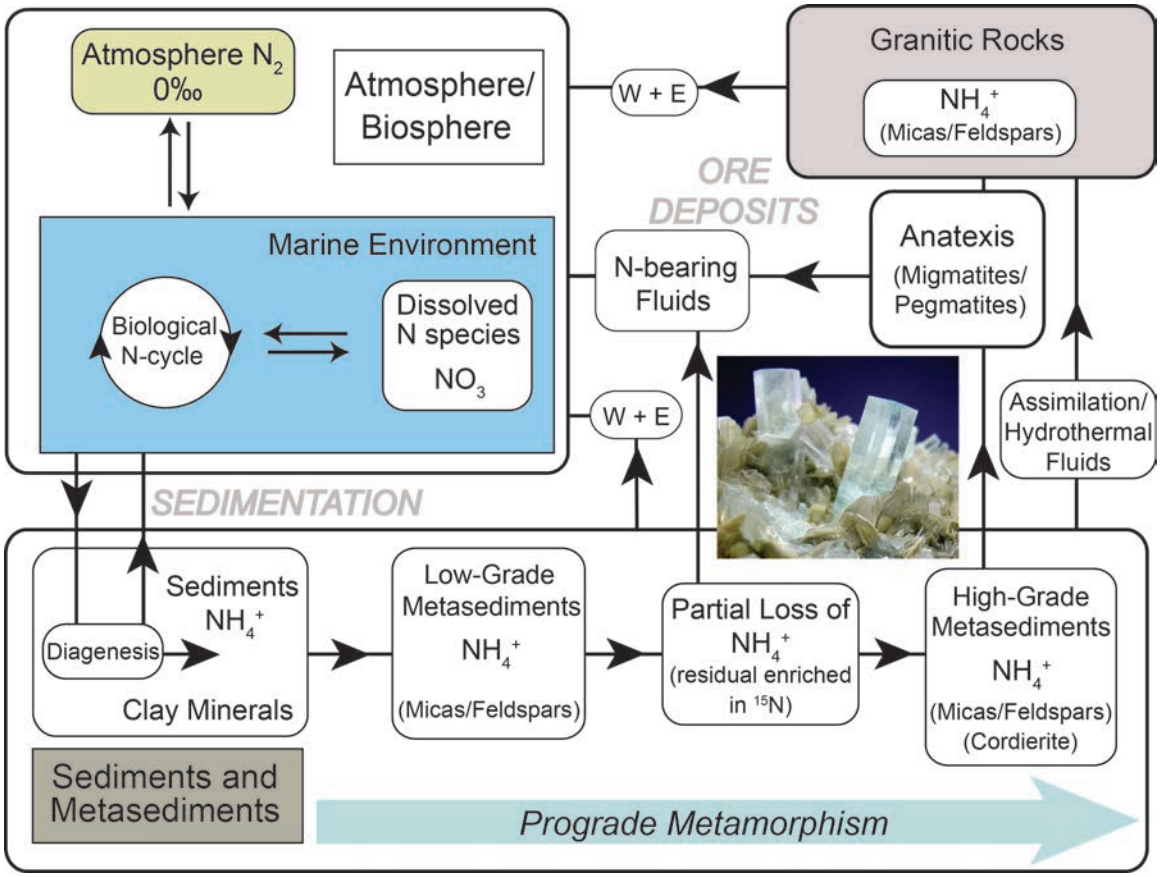
Atmosphere N_2
0‰
Atmosphere/
Biosphere
W + E
Granitic Rocks
NH_4^+
(Micas/Feldspars)
ORE
DEPOSITS
Marine Environment
Biological
N-cycle
Dissolved
N species
NO_3
N-bearing
Fluids
Anatexis
(Migmatites/
Pegmatites)
W + E
Assimilation/
Hydrothermal
Fluids
SEDIMENTATION
Sediments
NH_4^+
Diagenesis
Clay Minerals
Low-Grade
Metasediments
NH_4^+
(Micas/Feldspars)
Partial Loss of
NH_4^+
(residual enriched
in ^{15}N)
High-Grade
Metasediments
NH_4^+
(Micas/Feldspars)
(Cordierite)
Sediments and
Metasediments
Prograde Metamorphism

Figure 1

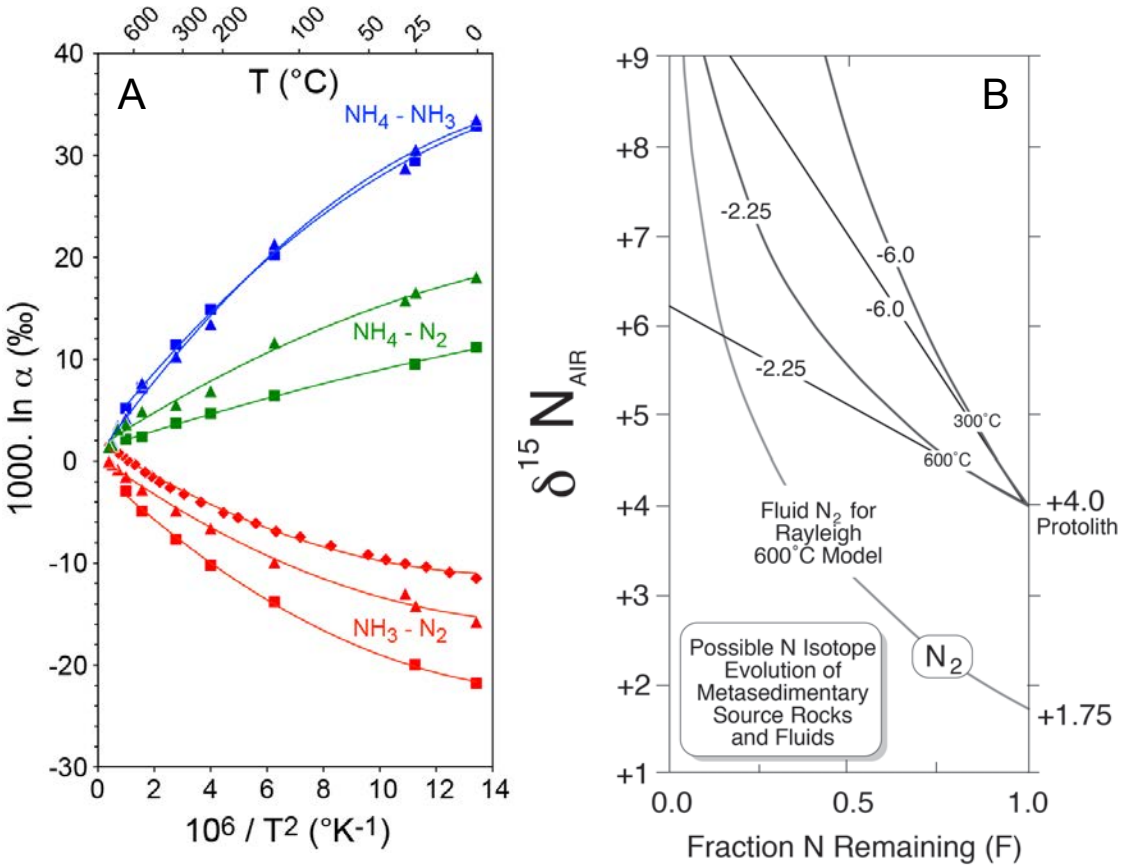
A
T (°C)
600
300
200
100
50
25
0
NH4 - NH3
NH4 - N2
NH3 - N2
1000. ln α (‰)
10^6 / T^2 (°K-1)
B
δ15NAIR
-2.25
-6.0
-6.0
-2.25
300°C
600°C
+4.0
Protolith
Fluid N2 for
Rayleigh
600°C Model
Possible N Isotope
Evolution of
Metasedimentary
Source Rocks
and Fluids
N2
+1.75
Fraction N Remaining (F)

Figure 2

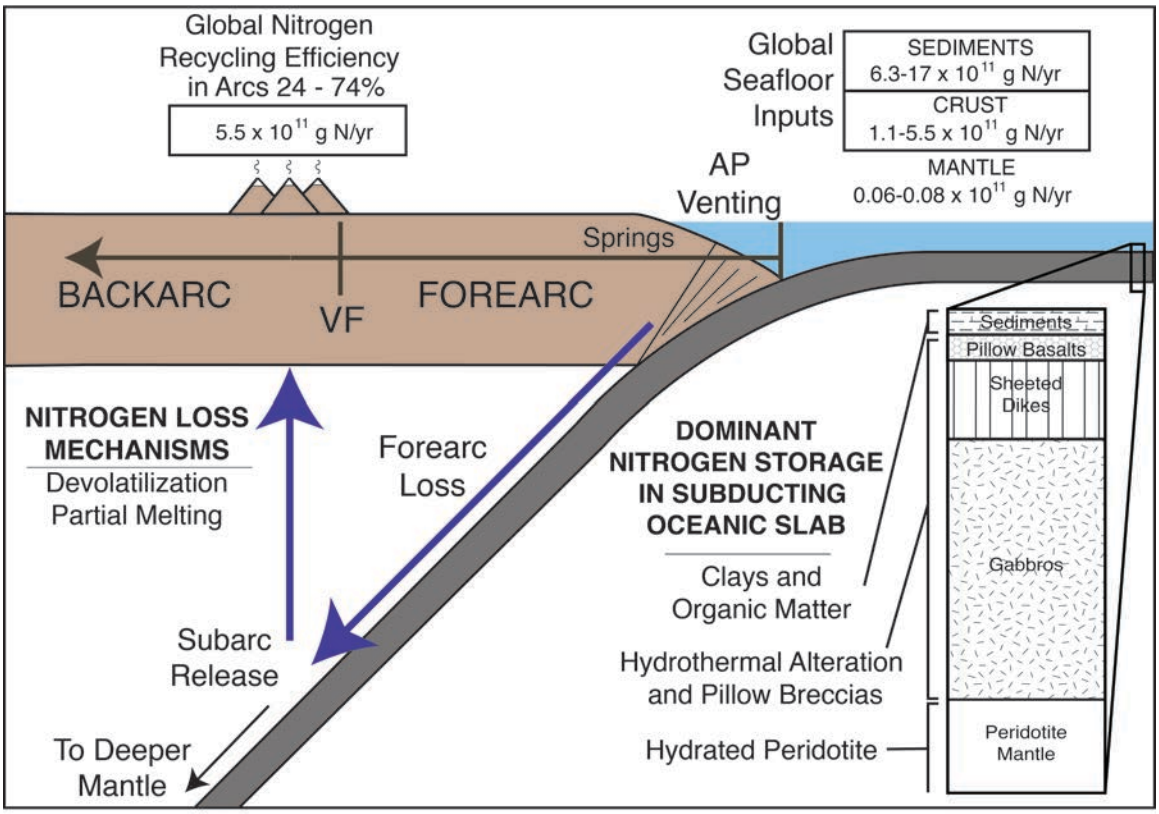
Global Nitrogen
Recycling Efficiency
in Arcs 24 - 74%
5.5 x 10^11 g N/yr
Global
Seafloor
Inputs
SEDIMENTS
6.3-17 x 10^11 g N/yr
CRUST
1.1-5.5 x 10^11 g N/yr
MANTLE
0.06-0.08 x 10^11 g N/yr
AP
Venting
Springs
BACKARC
VF
FOREARC
NITROGEN LOSS
MECHANISMS
Devolatilization
Partial Melting
Forearc
Loss
Subarc
Release
To Deeper
Mantle
DOMINANT
NITROGEN STORAGE
IN SUBDUCTING
OCEANIC SLAB
Clays and
Organic Matter
Hydrothermal Alteration
and Pillow Breccias
Hydrated Peridotite
Sediments
Pillow Basalts
Sheeted
Dikes
Gabbros
Peridotite
Mantle

Figure 3

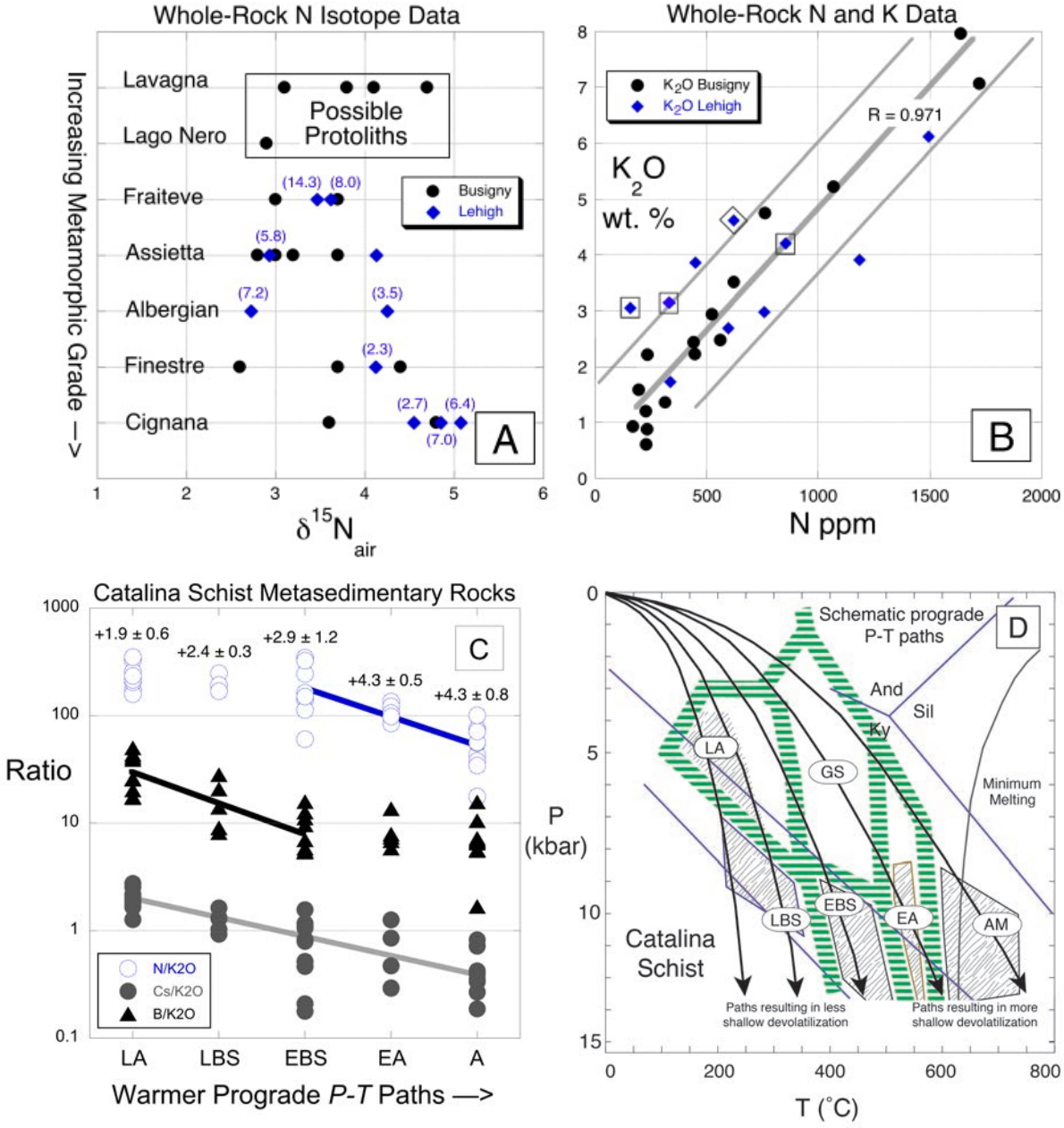
Whole-Rock N Isotope Data
Increasing Metamorphic Grade —v
Lavagna
Lago Nero
Fraiteve
Assietta
Albergian
Finestre
Cignana
Possible Protoliths
Busigny
Lehigh
(14.3) (8.0)
(5.8)
(7.2)
(3.5)
(2.3)
(2.7) (6.4)
(7.0)
A
δ15N air
Whole-Rock N and K Data
K2O Busigny
K2O Lehigh
R = 0.971
K2O wt. %
B
N ppm
Catalina Schist Metasedimentary Rocks
+1.9 ± 0.6
+2.4 ± 0.3
+2.9 ± 1.2
+4.3 ± 0.5
+4.3 ± 0.8
C
Ratio
N/K2O
Cs/K2O
B/K2O
LA
LBS
EBS
EA
A
Warmer Prograde P-T Paths —>
Schematic prograde P-T paths
D
And
Sil
Ky
LA
GS
Minimum Melting
LBS
EBS
EA
AM
Catalina Schist
Paths resulting in less shallow devolatilization
Paths resulting in more shallow devolatilization
P (kbar)
T (°C)

Figure 4

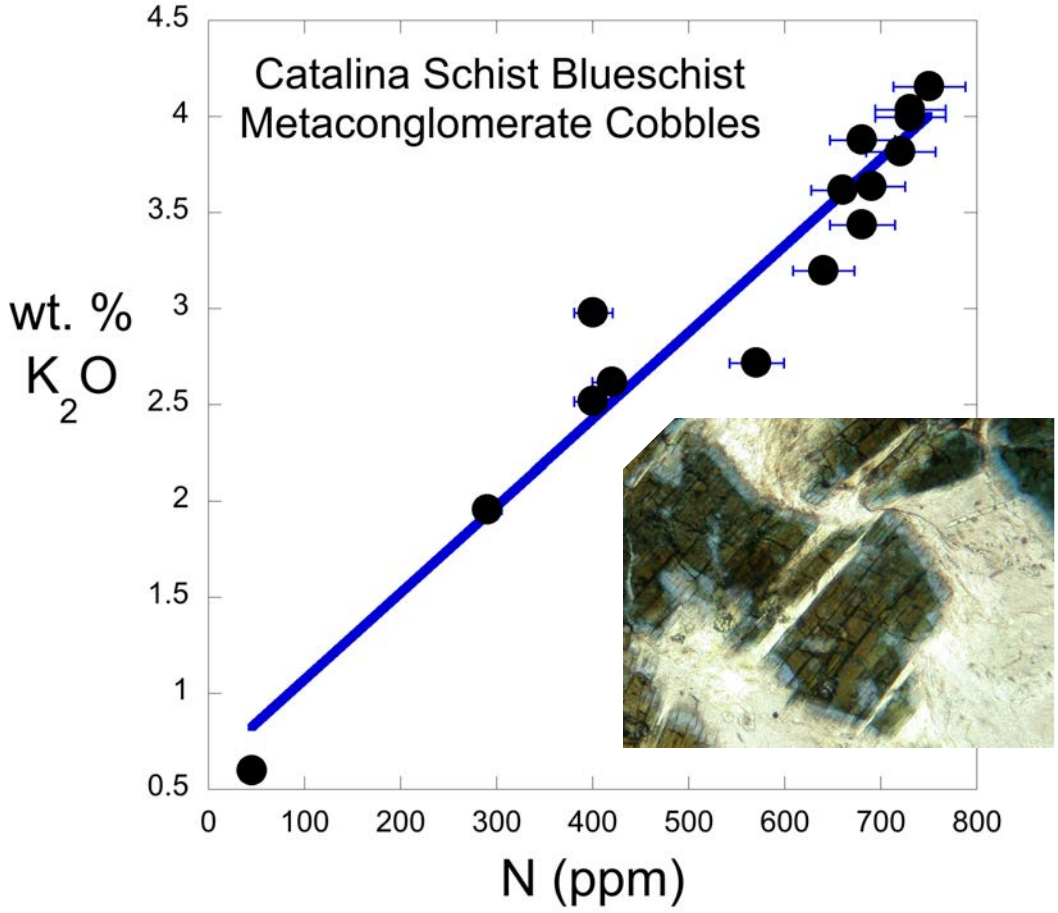
Catalina Schist Blueschist
Metaconglomerate Cobbles
wt. %
K2O
4.5
4
3.5
3
2.5
2
1.5
1
0.5
0
100
200
300
400
500
600
700
800
N (ppm)

Figure 5

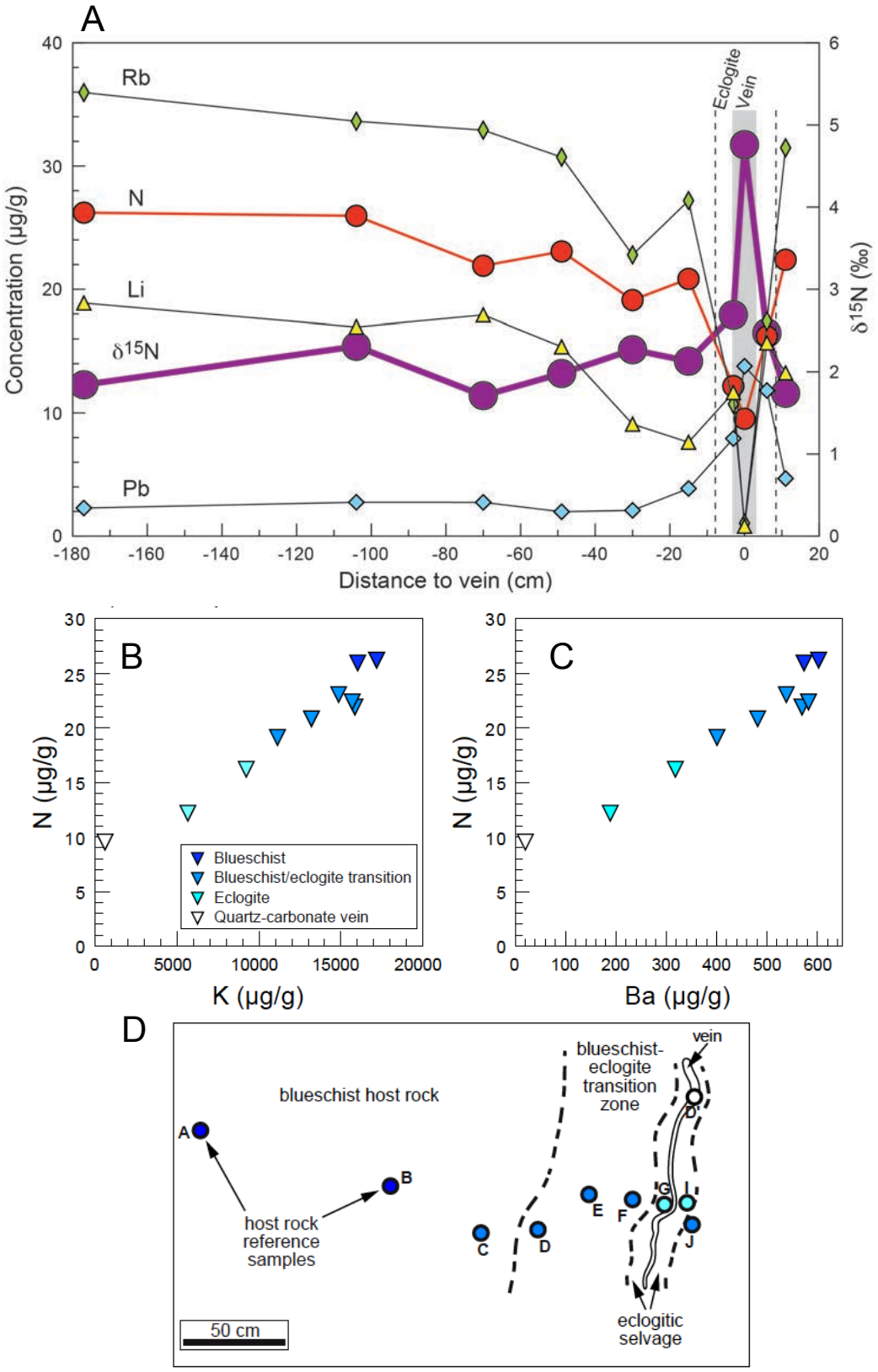
A
Rb
N
Li
δ15N
Pb
Eclogite Vein
Concentration (µg/g)
δ15N (‰)
Distance to vein (cm)
B
N (µg/g)
K (µg/g)
Blueschist
Blueschist/eclogite transition
Eclogite
Quartz-carbonate vein
C
Ba (µg/g)
D
blueschist host rock
blueschist-eclogite transition zone
vein
host rock reference samples
eclogitic selvage
50 cm

Figure 6

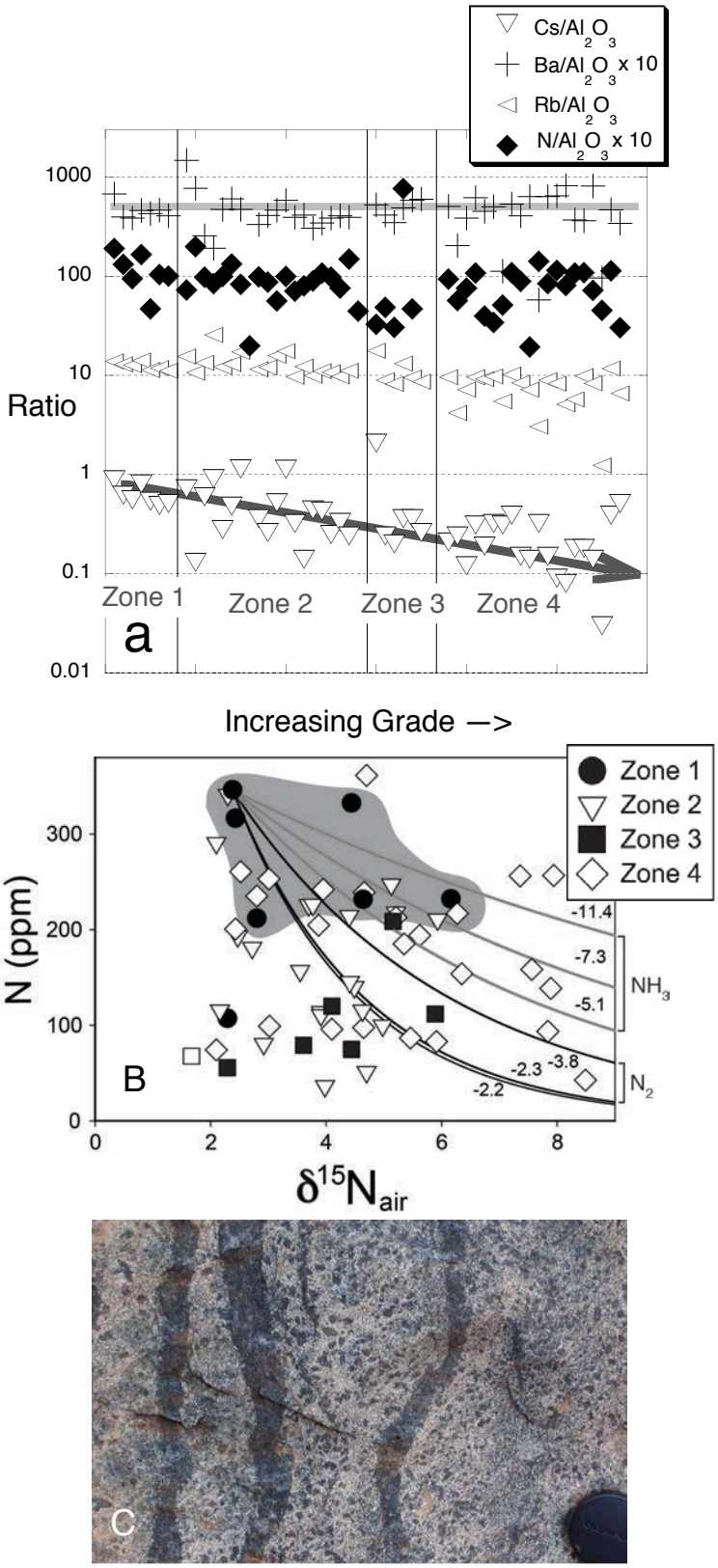
Cs/Al2O3
Ba/Al2O3 x 10
Rb/Al2O3
N/Al2O3 x 10
1000
100
10
1
0.1
0.01
Ratio
Zone 1
Zone 2
Zone 3
Zone 4
a
Increasing Grade —>
Zone 1
Zone 2
Zone 3
Zone 4
300
200
100
0
N (ppm)
-11.4
-7.3
-5.1
NH3
-2.3
-3.8
-2.2
N2
B
0
2
4
6
8
δ15Nair
C

Figure 7

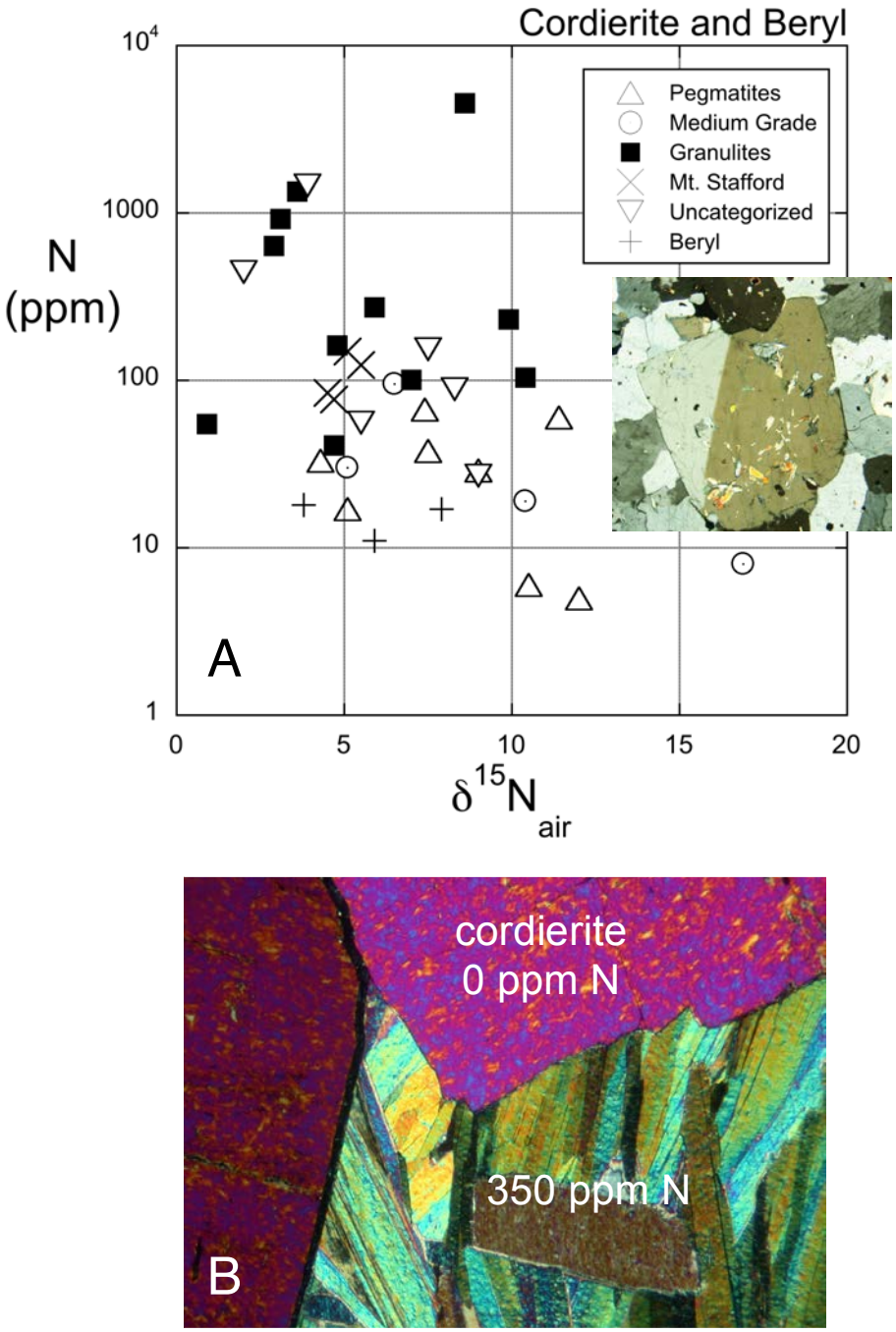
Cordierite and Beryl
Pegmatites
Medium Grade
Granulites
Mt. Stafford
Uncategorized
Beryl
N (ppm)
10^4
1000
100
10
1
0
5
10
15
20
$\delta^{15}N_{air}$
A
cordierite
0 ppm N
350 ppm N
B

Figure 8

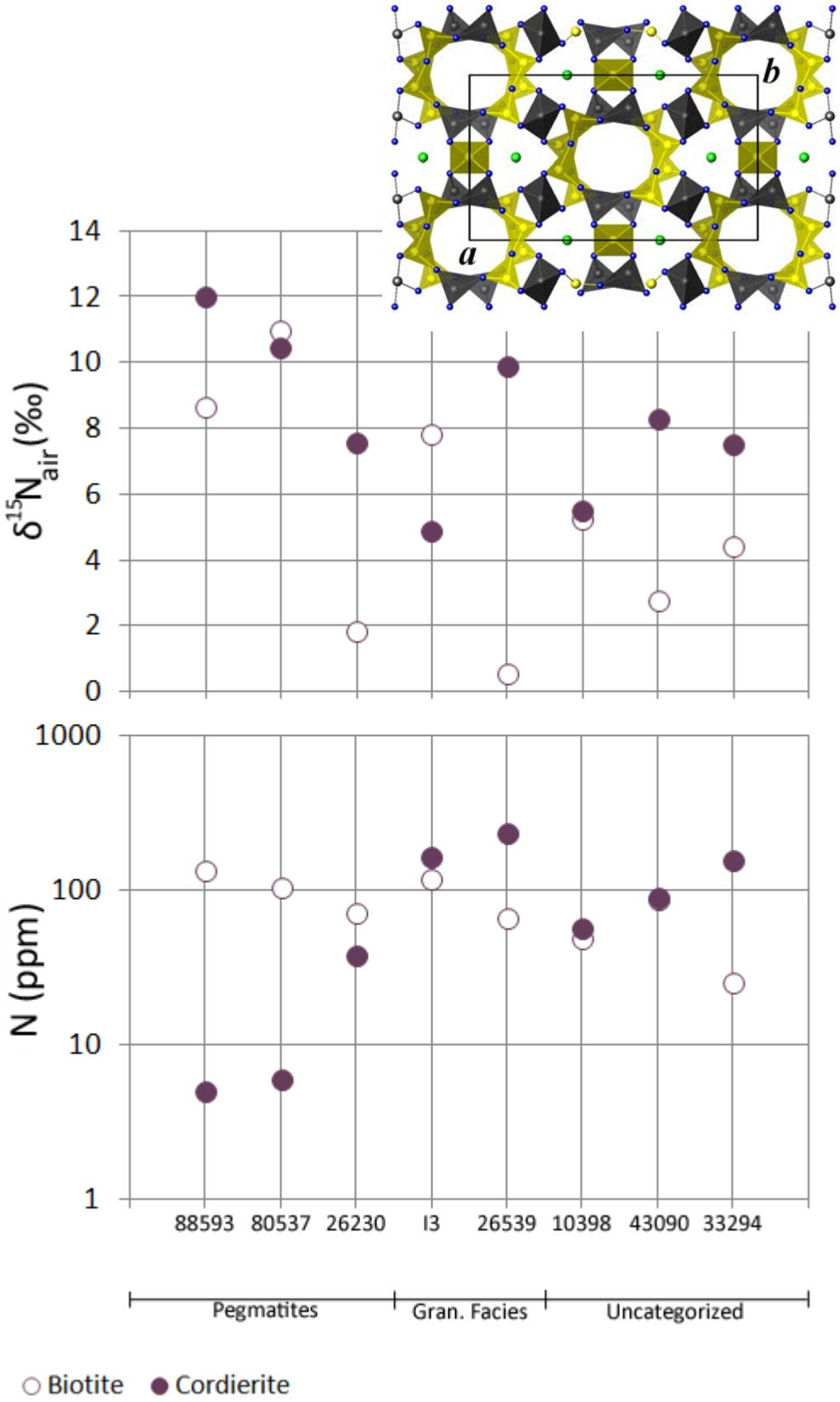
b
a
14
12
10
8
6
4
2
0
δ15Nair (‰)
1000
100
10
1
N (ppm)
88593
80537
26230
I3
26539
10398
43090
33294
Pegmatites
Gran. Facies
Uncategorized
Biotite
Cordierite

Figure 9

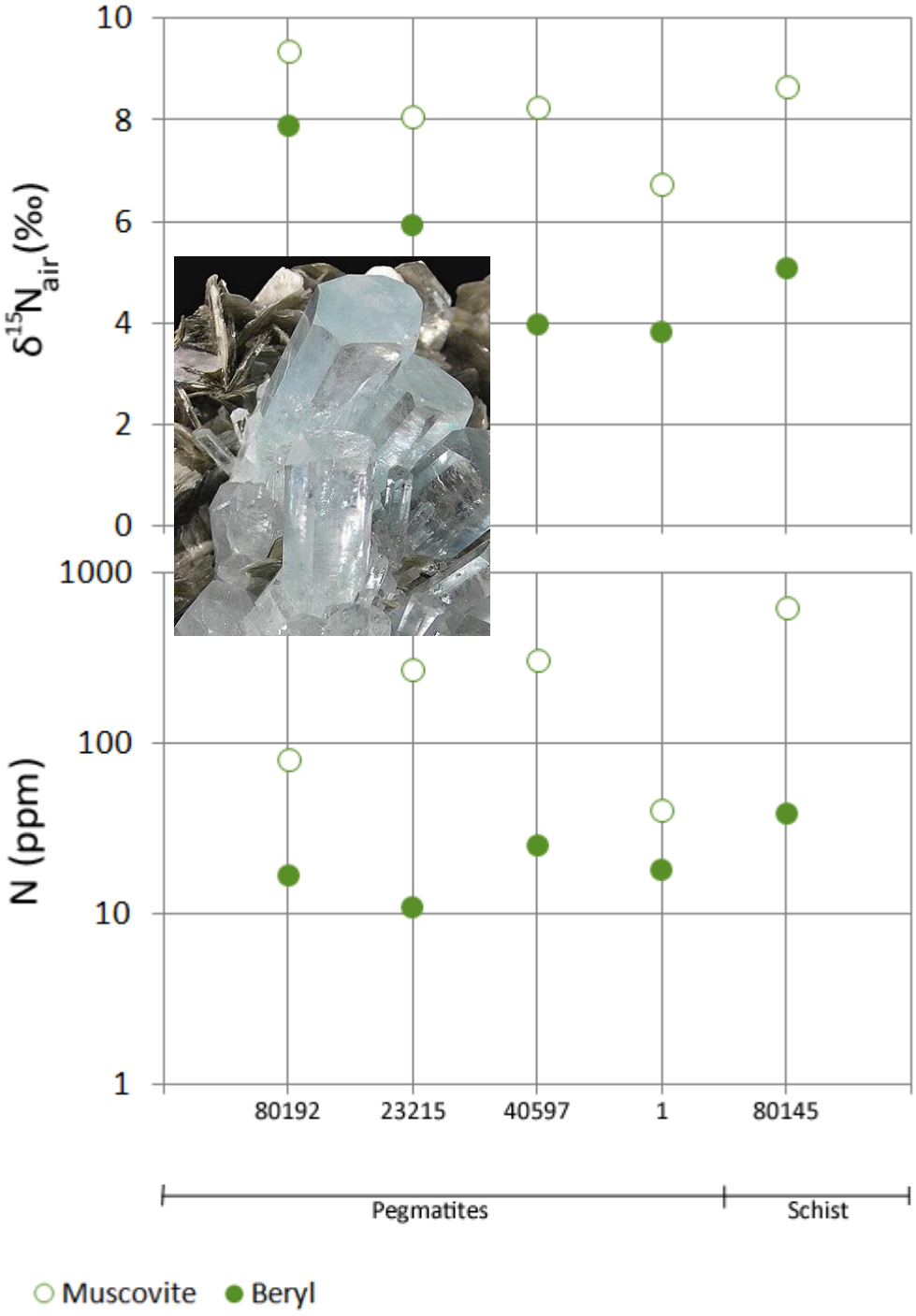
10
8
6
4
2
0
$\delta^{15}N_{air}$ (‰)
1000
100
10
1
N (ppm)
80192
23215
40597
1
80145
Pegmatites
Schist
Muscovite
Beryl

Figure 10

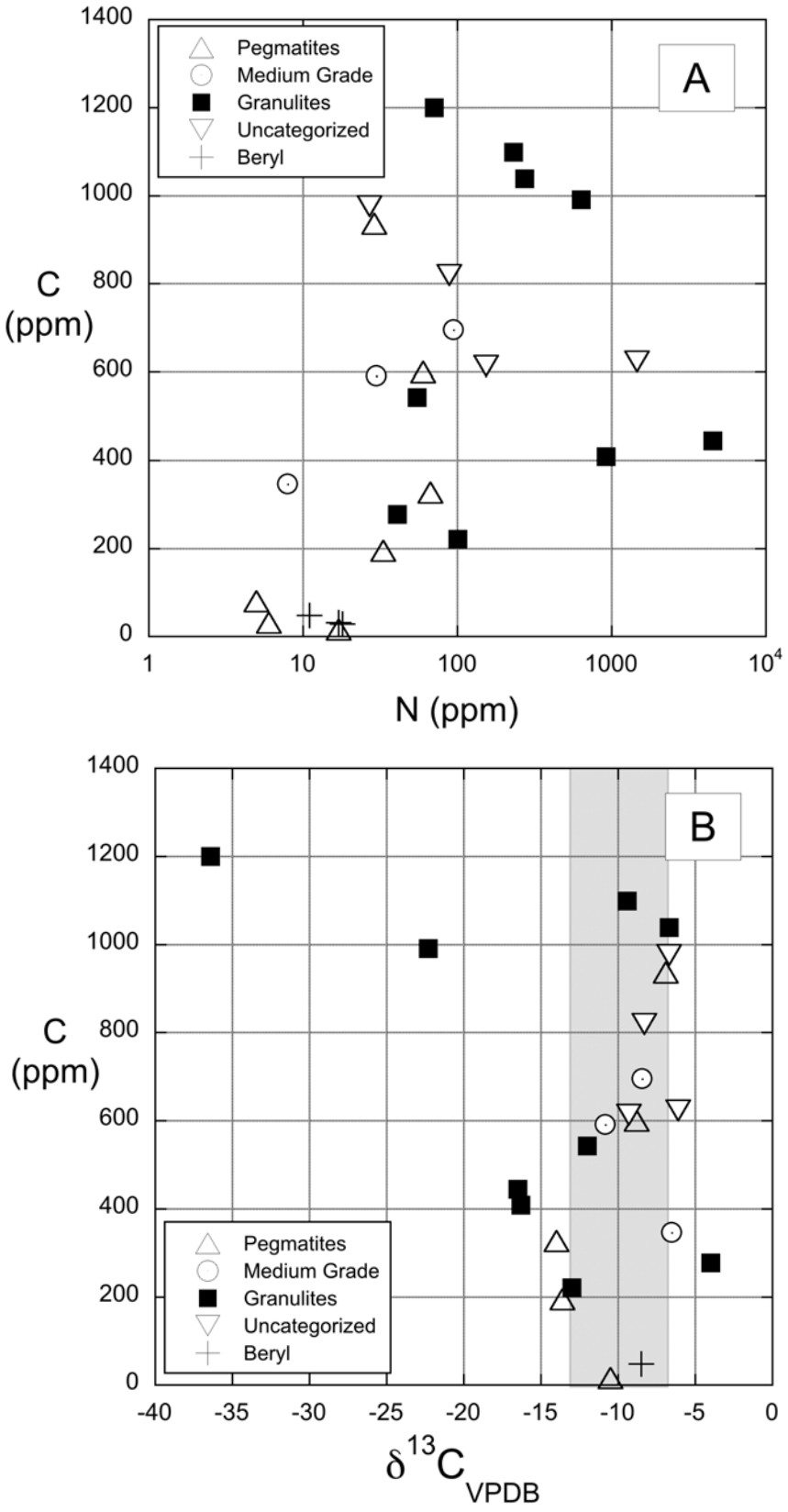
A
Pegmatites
Medium Grade
Granulites
Uncategorized
Beryl
C (ppm)
N (ppm)
1400
1200
1000
800
600
400
200
0
1
10
100
1000
10^4
B
C (ppm)
δ13CVPDB
-40
-35
-30
-25
-20
-15
-10
-5
0

Figure 11

Table 1. ESTIMATES OF THE MODERN-EARTH NITROGEN BUDGET, SHOWING THE VARIOUS RESERVOIRS, THEIR SIZES, AND THEIR PERCENT OF NITROGEN

	reservoir size 10^{21} g	% in reservoir
Goldblatt et al. (2009)		
Atmosphere	4	27.0
Continental Crust	2.1	14.2
Oceanic Crust	0.32	2.2
Mantle	8.4	56.7
TOTALS	**14.82**	**100**
Galloway (2003; surface/near-surface only)		
Atmosphere	3.95	79.5
Sedimentary rocks	1	20.1
Ocean N_2	0.02	0.4
Ocean NO_3^-	0.00057	0.01147
Soil organics	0.00019	0.00382
Land biota	0.00001	0.00020
Marine biota	0.0000005	0.00001
TOTALS	**4.97**	**100**

	reservoir size 10^{21} g	% in reservoir
Palya et al. (2011)[1]		
Atmosphere	3.9	29.3
Continental Crust	1.1	8.3
Oceanic Crust	0.32	2.4
Upper Mantle	0.17	1.3
Lower Mantle	7.8	58.7
Deep ocean	0.0006	0.00451
Surface ocean	0.00006	0.00045
Soils	0.0001	0.00075
Biomass	0.0000043	0.00003
Marine Biota	0.0000003	0.000002
Terrestrial vegetation	0.000004	0.00003
TOTALS	**13.29**	**100**

[1]Palya et al. (2011) and with estimates for oceanic crust from Li et al. (2007)

Table 2. Isotopic data for beryl and cordierite (and coexisting micas)

	Sample	Beryl $\delta^{15}N_{air}$	Beryl N (ppm)	Muscovite $\delta^{15}N_{air}$	Muscovite N (ppm)	$\Delta^{15}N_{mica\text{-}beryl}$	Beryl $\delta^{15}C_{VPDB}$	Beryl C (ppm)
Pegmatite/Partial Melts	80192	7.9	17	9.4	80	1.5		31
	23215	5.9	11	8.1	273	2.2	-8.5	48
	40597	4.0	25	8.3	305	4.3		
	1	3.8	18	6.7	41	2.9		28
	80145	5.1	39	8.7	632	3.6		

	Sample	Cordierite $\delta^{15}N_{air}$	Cordierite N (ppm)	Biotite $\delta^{15}N_{air}$	Biotite N (ppm)	$\Delta^{15}N_{mica\text{-}crd.}$	Cordierite $\delta^{15}C_{VPDB}$	Cordierite C (ppm)
Pegmatite/Partial Melts	88593	12.0	5	8.6	134	-3.4		80
	80537	10.5	6	11.0	103	0.5		31
	G-155a	5.1	17				-10.5	16
	C006	9.0	29				-6.9	936
	TUB-1	4.3	33				-13.6	195
	26230	7.5	38	1.8	70	-5.7		
	C004	11.4	60				-8.8	600
	84264	7.4	67				-14.0	327
Mid-grade Metamorphics	Wards	16.9	8				-6.5	345
	25 Geco Mine	10.4	19					
	WYO-2	5.1	30				-10.8	590
	118171	6.5	95				-8.4	694
Granulite Facies	X-1	4.7	41				-4.0	277
	42/IA	0.9	55				-12.0	543
	CL-177-1	30.0	71				-36.4	1200
	TA-5	7.0	101				-13.0	221
	129875	10.4	104					
	I3	4.8	162	7.8	116	3.0		
	26539	9.9	232	0.5	65	-9.4	-9.4	1099
	VS-1	5.9	273				-6.7	1039
	7114	2.9	634				-22.3	991
	S. India 1	3.1	923				-16.3	408
	89 V	3.6	1342					
	NE86A-24b	8.6	4525				-16.5	445
Uncategorized	CTSiM	9.0	27				-6.7	976
	10398	5.5	56	5.2	48	-0.3		
	43090	8.3	89	2.7	86	-5.5	-8.3	820
	33294	7.5	154	4.4	25	-3.1	-9.3	614
	H06	2.0	446					
	106886	3.9	1457				-6.1	623